Functional studies of

Influenza A virus NS1 protein

SHA Tim Wai

Table of contents

Abstract

The influenza A virus (IAV) is a problematic pathogen which affects both human health and the agricultural industry. IAV is a single, negative stranded and segmented RNA virus. Segment 8 of IAV encodes non-structural protein 1 (NS1) and nuclear export protein. NS1 was well characterised as a potent inhibitor of RIG-I mediated antiviral response in host cells. However, other roles of NS1 which are independent of RIG-I antagonism are less clarified. In this study, the roles of NS1 beyond RIG-I antagonism were extensively investigated. NS1-deficient IAV exhibited replication defect in cells deficient in RIG-I, which was rescued by exogenous expression of NS1 in cells. Moreover, complementation of NS1 in cells during infection also enhanced virus production. Furthermore, NS1 enhanced the packaging efficiency of the viral genome into IAV particles. Data from a virus like particle (VLP) production system demonstrated that NS1 also promoted packaging efficiency of an IAV reporter, composed of an antisense luciferase minigenome flanked by IAV untranslated regions. In line with a previous study which showed that NS1 acted as a structural component of virus particle, NS1 was also detected in IAV particles and VLP produced from NS1 expressing cells. A point mutation (R38A) in the dsRNA binding domain of NS1 failed to enhance virus production, genome packaging and NS1 incorporation. These results reveal a novel function of NS1 in facilitating viral genome packaging that is dsRNA binding dependent. Taken together, this study demonstrates the multifunctional properties of NS1, which optimises virus replication and infectivity not only through inhibition of RIG-I dependent antiviral response but also by promoting virus production and genome packaging, suggesting that NS1 is an attractive target for antiviral therapy for IAV infection.

Abbreviations

IAV: Influenza A virus

RdRP: RNA-dependent RNA polymerase

NS1: Non-structural protein 1

dsRNA: Double stranded RNA

vRNA: Genomic viral RNA

UTR: Untranslated region

RNP: Ribonuclear protein

HA: Haemagglutinin

M1: Matrix protein 1

KO: knock out

WT: wild type

IFN: Interferon

FFLuc: Firefly luciferase

VLP: Virus like particle

GFP: Green fluorescence protein

Chapter 1

Introduction

1.1 Background

Influenza A virus (IAV) is one of the most contagious pathogens which causes over 5 million infections globally per year. Both seasonal and pandemic influenza can cause huge impact to human health. The most iconic representative is the 1918 H1N1 Spanish flu, which infected almost one-fourth of the global population [1]. The high pathogenic avian influenza (HPAI) such as H5N1 also can cause huge economic damage to the agriculture industry. More importantly, because new influenza strains can emerge via genome recombination of influenza strains from different origins, HPAI is consistently regarded as a potential threat for pandemic influenza that can circulate through the human population.

1.2 IAV virology

IAV is a negative single-stranded RNA virus. Its viral genome is separated into eight individual segments and aligned in a 7+1 arrangement [2]. Each segment is composed of a negative-stranded RNA containing viral nucleoprotein (NP) monomers and a viral RNA-dependent RNA polymerase (RdRP) attached to panhandle end of RNA to form a ribonucleoprotein (RNP) complex [3]. To initiate an infection in cells, the viral haemagglutinin (HA) envelope protein on the surface of the virus particle first binds to sialic acid on cell surface glycoproteins and glycolipids [4]. The virus particle is then endocytosed and a fusion event occurs after HA has undergone a pH-dependent conformational change [4]. The viral RNPs are introduced in the cytoplasm and imported into the nucleus for replication. Newly replicated viral RNA is assembled as RNP in the nucleus and exported back to the cytoplasm [5]. These RNPs are further assembled with other viral structural proteins to form virus particles. Virus budding and release is driven by the neuraminidase (NA) protein which cleaves sialic acid groups on the cell surface [4].

1.3 IAV NS1 protein

Segment 8 of IAV encodes two proteins known as non-structural protein (NS1) and nuclear export protein (NEP) [6]. NS1 is a 26kD protein which consists of a double-stranded RNA (dsRNA) binding domain, an effector domain and a tail domain [6]. NS1 is a non-essential viral protein but plays critical roles for establishing efficient infection in hosts.

The innate immune response of host cells serves as the first line of defence to inhibit and control virus infection. The NS1 protein is a potent repressor of innate immune response. NS1 targets the cytoplasmic viral RNA sensor RIG-I, known to be a key initiator of type I interferon (IFN-I) production, upon virus infection [7]. NS1 targets RIG-I through a direct interaction of RIG-I CARD domain [8, 9]. NS1 also targets E3 ligase tripartite motif-containing protein 25 (TRIM25), which is a downstream protein of RIG-I, and inhibits the signal transduction leading to IFN induction [10, 11]. Besides RIG-I, NS1 also antagonises protein kinase R (PKR), which is a key inducer of cell death and inhibitor of viral protein synthesis [12, 13]. NS1 inhibits PKR through a direct binding to PKR and its upstream molecule interferon-induced protein kinase (PACT) [14, 15].

In addition to damping the host innate immune response, NS1 also interacts with and activates other host proteins which are potentially beneficial for virus replication. For example, NS1 can activate the phosphatidylinositol 3-kinase (PI3K)/ Akt pathway, which inhibits apoptosis and thus facilitates virus replication [16]. NS1 also interacts with cellular STAUFEN1 protein, which facilitates efficient viral mRNA translation [17].

The interaction between NS1 and host cellular factors attracts has thus attracted much scientific investigation. However, much less work has been done in

understanding its roles within the IAV particle itself. Some studies demonstrated that NS1 is a regulatory protein for viral gene expression [18-20]. Interestingly, a recent study showed that NS1 is incorporated in the virus particle. This observation challenges the classical view that NS1 is a non-structural protein [21]. However, how these phenotypes are placed in the context of viral life cycle and whether they have any implication to virus replication is not clear. In this study, the role of NS1 beyond IFN antagonism is investigated. My data shows that NS1 enhances M1 and HA synthesis, which result in increased virus production. Moreover, NS1 is involved in enhancing viral genome packaging, which facilitates the packaging of a complete sets of segments and optimise virus infectivity. Additionally, these phenotypes are dependent on the dsRNA binding domain of NS1. Identification of novel functions of NS1 increases the knowledge regarding the board-spectrum activities of IAV NS1.

Chapter 2

Materials and methods

2.1 Cells and viruses

Mardin-Darby canine kidney (MDCK) cells, HEK 293T WT and RIG-I KO cells [22] were cultured in Dulbecco's modified Eagle's medium (DMEM) (Nacalai Tesque) complemented with 5% foetal calf serum (FCS) (Gibco) and 1% penicillin and streptomycin (Nacalai Tesque). Cells were incubated at 37°C supplemented with 5% CO_2. Influenza A virus (A/PR/8/34 H1N1) wild type and recombinant virus delNS1 [23] were propagated in MDCK cells.

2.2 Sanger sequencing of A/PR/8/34 H1N1

Viral RNA was extracted by a QIAamp Viral RNA Mini Kit (QIAGEN) according to manufacturer's protocol. Complement DNA (cDNA) was synthesised by a High-Capacity cDNA Reverse Transcription Kit (ThermoFisher Scientific) using a Uni12 primer [24]. The cDNAs were further amplified by high fidelity PCR using a KOD-plus DNA polymerase (Toyobo) with published primer sets targeting individual segments of A/PR/8/34 H1N1 [24]. PCR products were purified by a Wizard™ SV Gel and PCR Cleanup System (Promega) and sequencing was performed by BigDye™ Terminator v3.1 Cycle Sequencing Kit (ThermoFisher Scientific) according to manufacturer's protocol. The sequences were analysed using an Applied Biosystems® 3500 Series Genetic Analyzer (ThermoFisher Scientific).

2.3 Generation of NS1 WT and NS1 R38A expression plasmids

The NS1 cDNA from A/PR/8/34 H1N1 was cloned to a pEF-Bos backbone expression plasmid (pEF-Bos NS1 WT) [25] with 5' EcoRI and 3' BamHI restriction sites. The NS1 R38A mutant expression plasmid was generated by high fidelity inverse PCR of pEF-Bos NS1 WT with primer set targeting NS1. The R38A nucleotide substitution was locate at the 5' end of forward primer. The PCR reaction was performed with a KOD-plus DNA polymerase (Toyobo) and the insert sequence

with mutation was validated by a BigDye™ Terminator v3.1 Cycle Sequencing Kit (ThermoFisher Scientific) according to manufacturer's protocol. The sequence was analysed using an Applied Biosystems® 3500 Series Genetic Analyser (ThermoFisher Scientific). The plasmids are propagated in Competent High DH5 (Toyobo) and purified using a QIAGEN Plasmid Kits (QIAGEN).

2.4 Cell transfection and infection

HEK 293T RIG-I KO cells were cultured in 6-well plates and washed once with phosphate buffered saline (PBS). Cells were then inoculated with PR8-delNS1 virus (MOI=0.01) suspended in PBS for 10 minutes on ice. The inoculum was then replaced with DMEM containing 5% FCS and 1% penicillin and streptomycin at 37°C with 5% CO_2 for 1 hour to initiate virus entry. Next, cells were transfected with 1µg of plasmid of interest by calcium phosphate precipitation mediated transfection according to a published protocol [26]. After 5 hours post transfection, medium was changed to DMEM supplemented with 0.2% bovine serum albumin (BSA) and 0.5 µg/ml of 6-(1-tosylamido-2-phenyl) ethyl chloromethyl ketone (TPCK)-treated trypsin (Sigma Aldrich). The cells were then incubated at 37°C and 5% CO_2 for a further 48 hours for virus replication.

2.5 Haemagglutination assay (HA assay)

A serial 2-fold dilution was prepared from a supernatant collected from virus-infected cells in a U-bottom 96-well plate. Next, 0.5% of chicken red blood cells (RBC) was added to the dilutions and incubated for 30 minutes at room temperature. The virus titre was determined as haemagglutination unit (HAU) which represents the dilution of the last well showing RBC agglutination (cloudy red).

2.6 RT-qPCR

Total RNA was extracted using a Trizol extraction protocol [27] and viral genomic RNA (vRNA) was extracted from supernatant of virus-infected cells using a QIAamp Viral RNA Mini Kit (QIAGEN) according to manufacturer's protocol. cDNA was synthesised from eight 5' tagged primers targeting individual eight segment of IAV vRNA using Superscript III reverse transcriptase (Invitrogen). The cDNA product was diluted 2-fold and subjected to qPCR using Thunderbird SYBR qPCR Mix (Toyobo) and StepOnePlus Real-Time PCR system (Applied Biosystems) with primer set targeting individual segment.

2.7 Virus purification

HEK 293T RIG-I KO cells were cultured in 10-cm dishes and infected with A/ PR/8/34 H1N1 (WT or delNS1). The supernatant was collected and centrifuged at low speed to remove cell debris after 48 hours post infection. Cell free supernatant was subsequently treated with RNAse A at 5 μg/ml for 1 hour at 37°C to remove any forms of RNA outside virus particle. Next, the supernatant was carefully layered on top of a cushion with 30% (w/v) sucrose in a PBS in a 30PA tube (Hitachi) and centrifuged at 141,000 × g for 2 hours at 4°C using a CP100NX ultracentrifuge (Himac) equipped with a P28S rotor. After centrifugation, the supernatant was removed and virus pellet was suspended in appropriate volume of PBS.

2.8 Western blotting

Cells or virus suspensions were lysed with 1% NP40 (Nacalai Tesque) in PBS supplement with protease inhibitor or 2X SDS sample buffer, respectively. Proteins were electro-blotted onto a polyvinylidene difluoride membranes (Millipore) at 100mA for 1 hour. The membrane was firstly blocked with 5% skimmed milk at room temperature for 30 minutes and incubated with anti-NP, anti-M1 (#sc-69824, Santa Cruz Biotechnology), anti-HA (#sc-52025, Santa Cruz Biotechnology) and ant-NS1

(#sc-130568, Santa Cruz Biotechnology) mouse monoclonal antibody (all in 1000-fold dilution in TBST) for overnight at 4°C. After incubation, the membrane was washed extensively using TBST and further incubate with goat anti-mouse IgG conjugated with horseradish peroxidase (2000-fold dilution in TBST) (Jackson ImmunoResearch) for 1 hour in room temperature. Finally, the membrane was treated with Chemi-Lumi One Super (Nacalai Tesque) and imaged using a LAS4000 (Fujifilm).

2.9 Urea PAGE

PR8-WT and PR8-delNS1 were propagated in MDCK cells and purified using ultracentrifugation (see 2.7). Genomic viral RNA from purified virus particle was extracted by Trizol and resuspended in RNAse free water. Equal amount of RNA was loaded and resolved on a 3% denaturing polyacrymide gel containing 7.5M urea (140V, 60 minutes). The gel was subsequently stained by a SYBR-Gold (Invitrogen) stain and exposed to UV for RNA visualisation. Images was acquired using a LAS4000 (Fujifilm).

2.10 vRNA-FISH

293T RIG-I KO cells were grown on poly-D lysine-coated coverslips to approximately 30% confluency. After virus infection and transfection, cells were fixed with 4% paraformaldehyde for 10 minutes and permeabilised with 0.5% Triton X-100 in PBS for 15 minutes. RNA fluorescence in situ hybridisation (RNA FISH) using a QuantiGene ViewRNA ISH Cell Assay Kit (Affymetrix) was performed on the fixed cells according to the manufacturer's protocols. In brief, the cells were incubated with a probe set targeting negative strand segment 5 (#VF1-1058) at 100-fold dilution for 3 hours at 40°C. Sequential incubations were performed with pre-amplifier, amplifier and label probe (all 25-fold dilution) for 30 minutes at 40°C. The

processed cover slips were either stored at 4°C in PBS or proceed to immunofluorescence staining.

2.11 Immunofluorescence staining

Coverslips with fixed cells or FISH processed cells were incubated in a blocking buffer (PBS/2% BSA) overnight. Primary antibodies were incubated with either mouse monoclonal anti-M1 (200-fold dilution in blocking buffer) (#sc-69824, Santa Cruz Biotechnology) or anti-HA (200-fold dilution in blocking buffer) (#sc-52025, Santa Cruz Biotechnology) combined with rabbit polyclonal anti-NS1 (500-fold in blocking buffer) (#GTX125990) antibody for 1 hour at room temperature. Primary antibodies were then removed from coverslips and washed three times with PBS followed by treatment of Alexa Fluor 647 Donkey anti-Mouse IgG H+L (#A-31571, Invitrogen) and Alexa Fluor 488 donkey anti-rabbit IgG H+L (#A-21206, Invitrogen) supplemented with 1 µg/ml of DAPI to stain nuclei (all at a 1000 dilution in blocking buffer) for 1 hour at room temperature. Coverslips were washed three times with PBS and mounted with Fluoromount-G (SouthernBiotech). The coverslips were observed under a confocal laser scanning microscope TCS-SP8 (Leica Microsystems).

2.12 VLP production system

VLPs were generated as described previously [22]. In brief, HEK 293T RIG-I KO cells (donor cells) in 6-well plates were co-transfected with 2 µg of the pCAGGS-M1; 1 µg of pCAGGS-HA, NA, NP, PB1, PB2 and NEP; 0.1 µg of pCAGGS-PA and M2; 1 µg of a firefly luciferase-encoding minigenome flanked with segment 5 or 8 UTR in a negative orientation, and 0.75 µg of pRL-SV40 (Renilla luciferase for internal control) in the presence or absence of pEF-Bos NS1, using calcium phosphate precipitation mediated transfection. After 48 hours post transfection,

supernatants were treated with 25 U/ml of Benzonase nuclease (Novagen) for 3 hours at 37°C to remove excess plasmids which were remained in the supernatant. The supernatants were then incubated with fresh HEK 293T WT and RIG-I KO cells (recipient cells) which were pre-transfected with 1 μg of pCAGGS-NP, PB1 and PB2, and 0.1 μg of pCAGGS-PA in 96 well plate. After 8 hours post incubation, donor cells and recipient cells were lysed in 1x Passive Lysis Buffer (Promega) and the luciferase quantity was measured using the Dual-Luciferase Reporter System (Promega) with a Lumat LB 9507 luminometer (Berthod Technologies). Relative luciferase units were read as fold induction relative to the mock control in which pCAGGS-PB2 was not included in the co-transfected recipient cells. For immunofluorescence, recipient cells were stained with a mouse monoclonal anti-luciferase antibody (200-fold dilution in blocking buffer) (#sc-74548, Santa Cruz Biotechnology) for 1 hour at room temperature and followed by incubation of Alexa Fluor 647 Donkey anti-Mouse IgG H+L (1000-fold dilution with blocking buffer) (#A-31571, Invitrogen) for 1 hour at room temperature. For VLP purification, supernatant was layered on a cushion with 20% (w/v) sucrose in PBS in 30PA tube (Hitachi) and centrifuged at 141,000 × g for 2 hours at 4°C using a CP100NX ultracentrifuge (Himac) equipped with a P28S rotor. Supernatant was removed and VLP pellet was suspended in appropriate volume of PBS.

2.13 Statistical analysis

Statistical analysis was performed using Prism 6 software (GraphPad). The Student's two-tailed t-test was used to compare two groups and one-way ANOVA followed by Tukey's test was used for multiple comparisons. Unless specified, data was expressed as mean ± SD with $P<0.05$ being considered significant (*$P<0.05$, **$P<0.01$)

Chapter 3

Results

3.1 HEK 293T RIG-KO cell is incapable of inducing IFN in virus infection

To study the function of NS1 protein, a recombinant virus delNS1 in which the NS1 open reading frame is deleted and hence NS1 protein is not expressed throughout the virus life cycle, was used (Fig 3.1-A). First, the phenotype of delNS1 virus was examined. HEK 293T WT cells were infected with PR8-WT, PR8-delNS1 and Sendai virus (SeV), which is a well-established stimulator of host cell antiviral signalling. RNA was extracted from virus-infected cells and IFN-β mRNA was quantified by RT-qPCR. As expected, while mock and PR8-WT infected cells produced a comparable amount of IFN-β mRNA, both PR8-delNS1 and SeV infected cells produced significantly high amount of IFN-β mRNA (Fig 3.1-B). In contrast, HEK 293T RIG-I KO cells, which lack the cytoplasmic viral RNA sensor RIG-I, were not capable of producing IFN-β under virus infection (Fig 3.1-B). This result agrees with reports showing that NS1 is a potent antagonist of RIG-I antiviral signalling [8, 28-30].

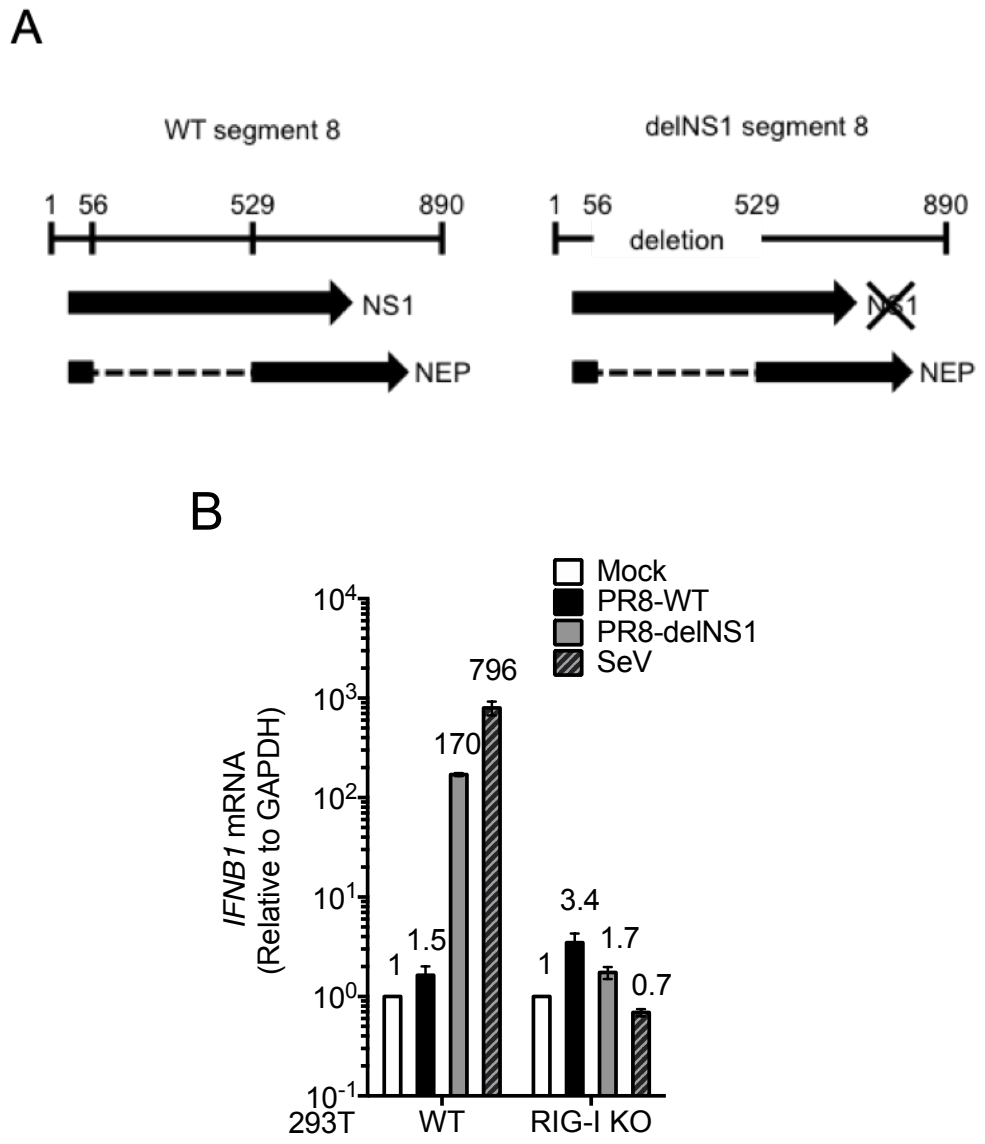

Fig 3.1 Phenotype of PR8-delNS1 and HEK 293T RIG-I KO cells

(A) Comparison of segment 8 genome of between PR8-WT and PR8-delNS1. The open reading frame of NS1 (nucleotide position 56-529) were deleted in segment 8 of delNS1 such that NS1 is not expressed but the spliced product NEP expression was unaffected. (B) HEK 293T WT and RIG-I KO cells were infected with PR8-WT, PR8-delNS1 or SeV at MOI=0.1. After 24 hours post infection, cellular total RNA was extracted and reverse transcribed by random primers. Level of mRNA expression was determined using qPCR with primer set targeting IFNB1. The data represents the mean ± standard deviation from two independent experiments (n=2).

3.2 PR8-delNS1 replicate inefficiently compared to PR8-WT in innate immune incompetent RIG-I KO cell.

Next, the antiviral effect of IFN-β on virus replication was examined. Supernatant was collected from virus-infected HEK 293T WT cells and virus titre was determined via plaque assay. As expected, PR8-delNS1 virus replicated poorly in WT cells compare to PR8-WT virus due to the presence of IFN-β (Fig 3.2-A). For RIG-I KO cells, interestingly, the titre of PR8-delNS1 was partially recovered but remained significantly attenuated compare to PR8-WT regardless the absence of IFN-β (Fig 3.2-B). This result suggests that NS1 possess additional function, which is necessary for optimal virus replication, besides antagonising host cell antiviral response.

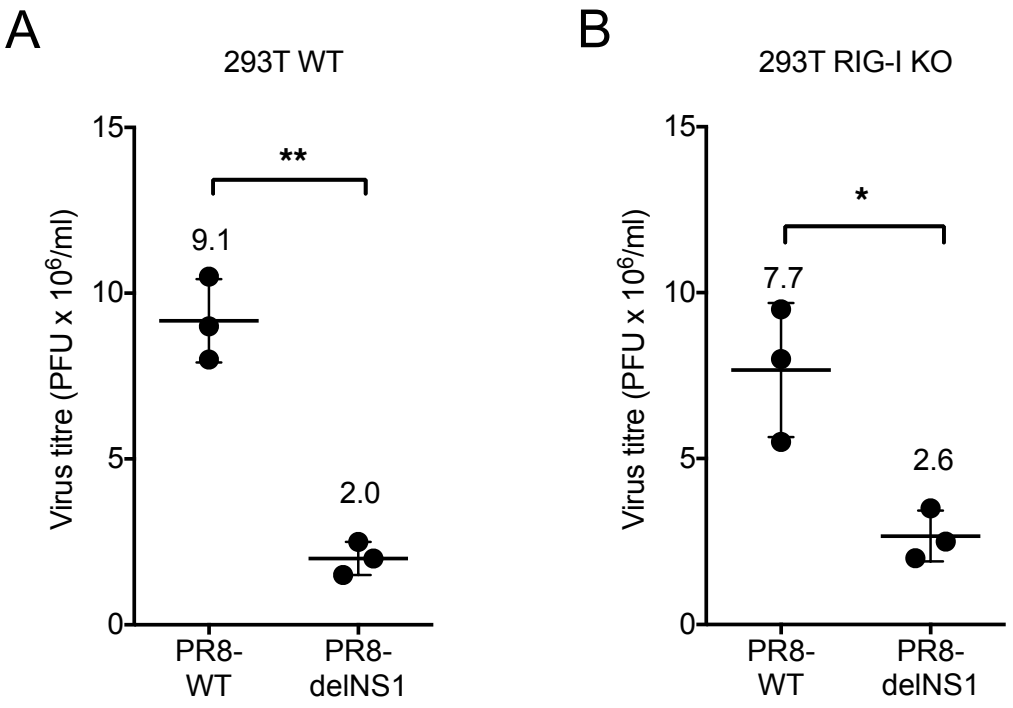

Fig 3.2 Replication of PR8-WT and PR8-delNS1 in HEK 293T WT and RIG-I KO cells

(A) HEK 293T WT cells and (B) HEK 293T RIG-KO cells were infected with either PR8-WT or PR8-delNS1 at MOI=0.01. After 48 hours post infection, virus titre was determined by plaque assay using MDCK cells. The data represents the mean ± standard deviation from at least three independent experiments (n=3). The Student's t test was used for statistical analysis (**P<0.01, *P<0.05).

3.3 PR8-WT and PR8-delNS1 possess different genomic sequence.

For RNA viruses including influenza A virus, due to the low fidelity of RNA-dependent RNA polymerase, random point mutations often arise during genome replication [31]. Base on this, it is possible that PR8-WT and PR8-delNS1 could accumulate mutations differently through multiple propagation during virus stock preparation. To address this, the full sequence of the both viruses were determined by Sanger sequencing. Multiple point and silent mutations were observed in all genome segments in PR8-delNS1 when compared against PR8-WT (Table 3.3). Moreover, segment 4, which encodes HA protein, contained an in-frame deletion (nucleotide position 471-473) and the sequence differ the most between PR8-WT and PR8-delNS1. Least difference was observed in segment 5, which encodes NP protein.

Segment 1 (PB2)	
Nucleotide change	Amino acid change
c342u	M105I
u630c	No change
c1245u	No change
a1269g	No change
c1527a	No change
u1537c	I504V
c1705u	V560I
g2001a	No change
u2088c	No change
g2109a	No change
c2132u	R702K
a2149g	No change
u2238c	No change

Segment 2 (PB1)	
Nucleotide change	Amino acid change
g99a	No change
u294c	No change
u297c	No change
c435u	No change
u563c	E180G
u639c	I205M
c647u	R208K
c1015u	E331K
u1217c	E398G
u1311c	No change
a1401g	No change
u1594c	S524G
u2076c	No change

Segment 3 (PA)	
Nucleotide change	Amino acid change
u53c	N10S
c326u	G101E
a339g	No change
g765a	No change
g795a	No change
g848a	P275L
c867u	No change
g1629a	No change
g1672u	L550I
u2034c	No change
c2052a	No change
c2068u	D682N
u2106c	No change

Segment 4 (HA)	
Nucleotide change	Amino acid change
u143g	No change
u225c	T65A
a245u	N71K
u380c	No change
u383c	No change
471-473	In frame deletion
g499(496)u	A156(155)E
c587(584)u	No change
c597(584)u	No change
a630(627)g	S200(199)P
c838(835)a	R269(268)M
c862(859)u	G277(276)D
c899(896)u	M289(288)I
a958(955)u	F309(308)I
u1080(1077)a	I350(349)F
a1100(1097)c	No change
c1205(1202)u	No change
a1224(1221)u	S398(397)T
g1246(1243)a	T405(404)I
u1279(1276)g	K416(415)T
c1511(1508)u	M493(492)I
u1749(1746)c	No change

Segment 5 (NP)	
Nucleotide change	Amino acid change
a186g	No change
g837a	No change
c905u	S287N
c1102g	V353L
g1334u	T430N

Segment 6 (NA)	
Nucleotide change	Amino acid change
u63g	M15L
u101c	No change
g109a	T30I
a146g	No change
a199g	I60T
g213u	P65T
c403u	R128K
u412c	N131S
c731u	No change
c881u	No change
u960c	K314E
u1211c	No change
u1229c	I403M
a1337g	No change
g1372c	T451S

Segment 7 (M)	
Nucleotide change	Amino acid change
a58u	No change
u97g	No change
g270u	T82N
c434u	A137T
c463u	No change
c523a	No change
c655u	No change
c792u	A27T

Segment 8 (NS)	
Nucleotide change	Amino acid change
u21c	No change
a33u	S3P
56-528	In frame deletion
u575(117)c	E26G
c578(120)u	G27D
c763(305)u	V89I
u849(391)c	No change
u865(406)c	No change

Legend:
- u(Nucleotide, PR8-WT) 225(Position) c(Nucleotide, PR8-delNS1)
- T(Amino acid, PR8-WT) 65(Position) A(Amino acid, PR8-delNS1)
- 471-473 (in frame deletion in delNS1)

Table 3.3 Comparison of complete viral genome sequence of PR8-WT and PR8-delNS1

Viral RNA was extracted and reverse transcribed using Uni13 primer. The cDNA was amplified using primer set targeting individual 8 segments determined by Sanger Sequencing.

u(Nucleotide of PR8-WT) 225(Position) c(Nucleotide of PR8-delNS1); T (Amino acid code of PR8-WT) 65(Position) A(Amino acid code of PR8-delNS1); 471-473 (in frame deletion in PR8-delNS1)

3.4 NS1 optimise virus infectivity and virus production independent of RIG-I antagonism.

In order to rule out the factor of viral genome difference between PR8-WT and PR8-delNS1 shown in Table 3.3, a transient transfection-based rescue experiment was performed to address whether NS1 is specifically required for enhancing virus replication independent of its ability to antagonising RIG-I mediated antiviral response which was observed in Fig 3.2-B. HEK 293T RIG-I KO cells were first infected with PR8-delNS1 virus and subsequently transfected with an empty control plasmid (E.C), a GFP or a NS1 expression plasmid. After an incubation period, supernatant was collected and virus titre was determined by plaque assay. As expected, virus titre of both E.C. and GFP expressing cells were comparable to mock transfected cells. Strikingly, a significantly high level of virus titre was detected in NS1 expressing cells (Fig 3.4-A). This suggests that NS1 can enhance infectivity of PR8-delNS1 virus.

The increase of virus titre suggests that more infectious virus particles are produced from these NS1 expressing cells. To show this, same volume of purified virus fraction was prepared from supernatant and the level of viral structural proteins (NP, M1 and HA) were determined by Western blot. A higher level of structural proteins was detected in virus fraction from NS1 expressing cells. The difference was more dramatic in M1 and HA2 (cleaved HA) protein level (Fig 3.4-B, Purified virion). Previous studies showed that NS1 regulates viral gene expression and protein translation in an infected cell [18, 20]. Western blot of cell lysate from NS1 expressing virus-infected cells showed that level of M1 and HA2 protein but not NP was highly upregulated (Fig 3.4-B, Infected cells). Confocal microscopy clearly demonstrated that within an individual cell, M1 and HA protein were highly expressed

in the presence of NS1 (Fig 3.4-C). In addition to Western blot, haemagglutinin assay (HA assay) revealed that NS1 expressing cells produced approximately 2-fold more virus particle (expressed as HAU/50μl) than E.C. expressing cells. (Fig 3.4-D).

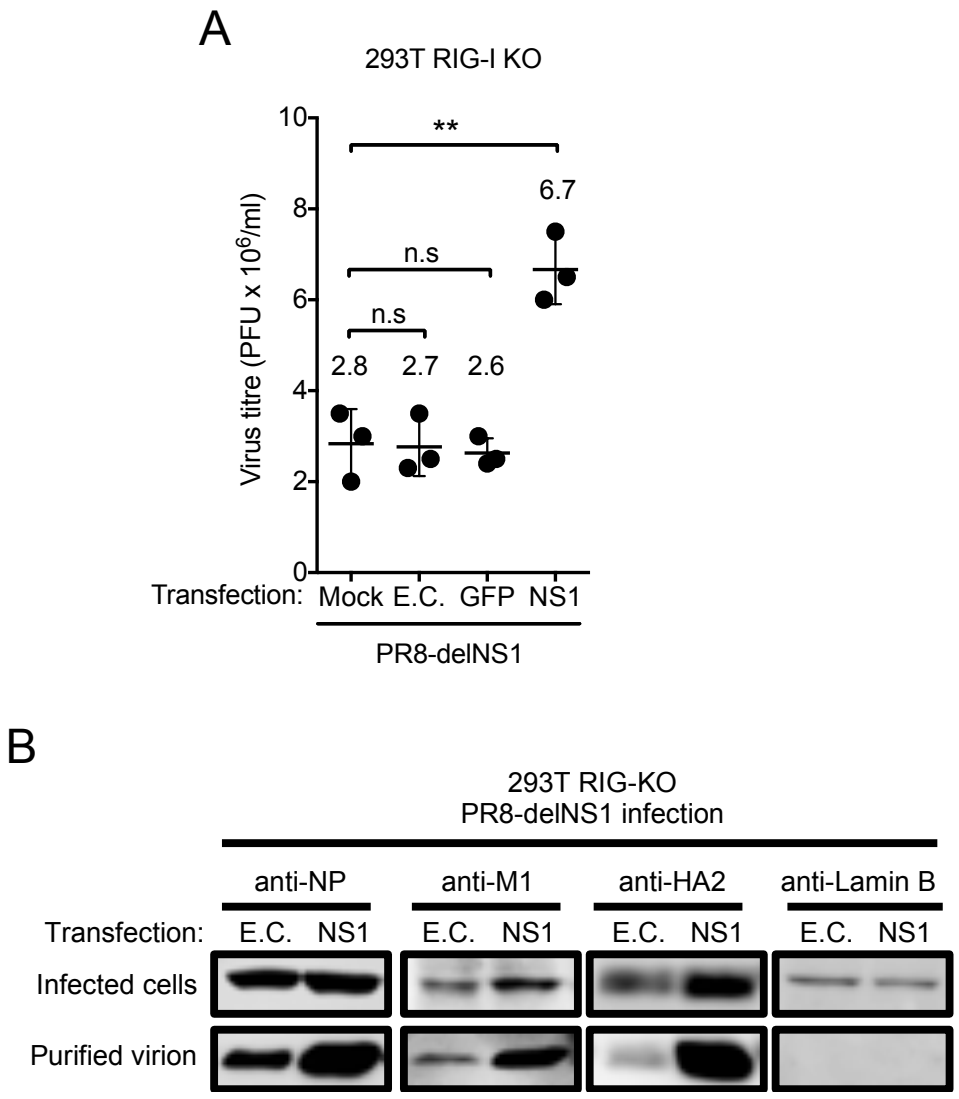

Fig 3.4 Examination of the effect of exogenous NS1 expression on PR8-delNS1 infectivity and virus production.

(A) HEK 293T RIG-I KO cells were infected with PR8-delNS1 virus and transfected with pEF-Bos NS1 and control plasmids (Empty control (E.C.) or GFP). After 48 hours post infection, virus titre was determined using MDCK cells. The data represents the mean ± standard deviation from at least three independent experiments (n=3). The one-way ANOVA followed by Tukey's test was used for statistical analysis (n.s. not significant, **P<0.01). (B) Cell lysate and equal volume of purified virion suspension were subject to SDS-PAGE and protein amount was determined using anti-NP, anti-M1, anti-HA2 (cleaved HA) and anti-Lamin B antibodies.

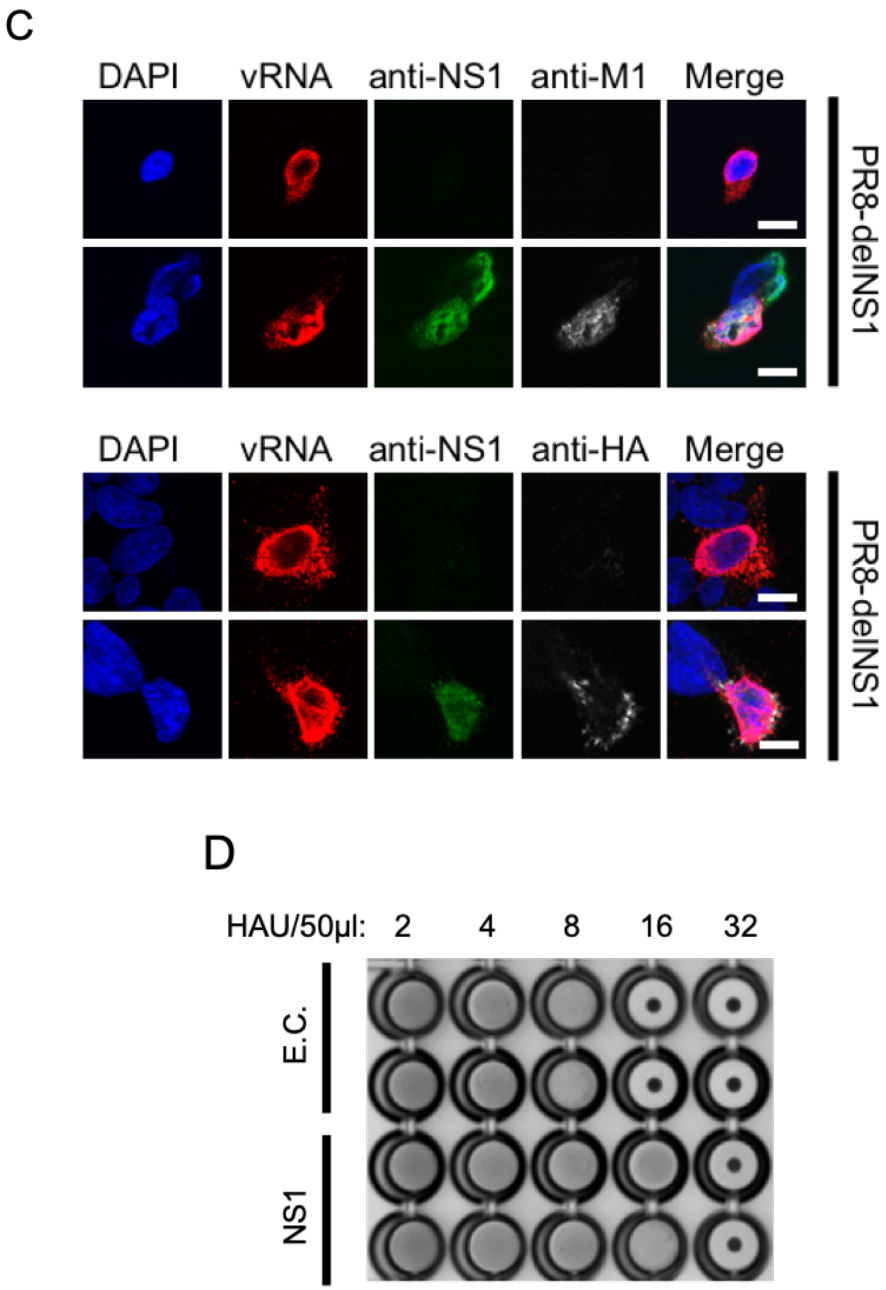

Fig 3.4 Examination of the effect of exogenous NS1 expression on PR8-delNS1 infectivity and virus production.

(C) HEK 293T RIG-I KO cells were infected with PR8-delNS1 at MOI=0.1 and transfected with pEF-Bos-NS1 or control plasmids. After 24 hours post infection, cells were stained with an RNA FISH probe targeting segment 5 viral genomic RNA (Red), anti-NS1 (Green), anti-M1, anti-HA antibodies (White) and DAPI (Blue). Scale bar 10 µm. (D) Virus titre (HAU/50µl) was determined from supernatant collected from (A) using HA assay.

3.5 NS1 is pre-packaged within the virus particle

NS1 is initially classically considered as a non-structural protein. However, Western blot revealed that a significant amount of NS1 was present in purified virion fractions produced from NS1 expressing cells (Fig 3.5-A, Purified virion). A similar result was obtained using purified virion fraction prepared from PR8-WT virus-infected cells indicating that incorporation of NS1 into the virion was not an artefact of over-expression of NS1 (Fig 3.5-B, Purified virion). Lamin B was undetected in virus fraction, demonstrating that there was no contamination of cellular protein during the purification process (Fig 3.5-B, Purified virion). Furthermore, the virion-associated NS1 was sensitive to trypsin digestion after disruption of the virus envelope by triton (Fig 3.5-C). This result suggests that NS1 is likely packaged within the virus particle.

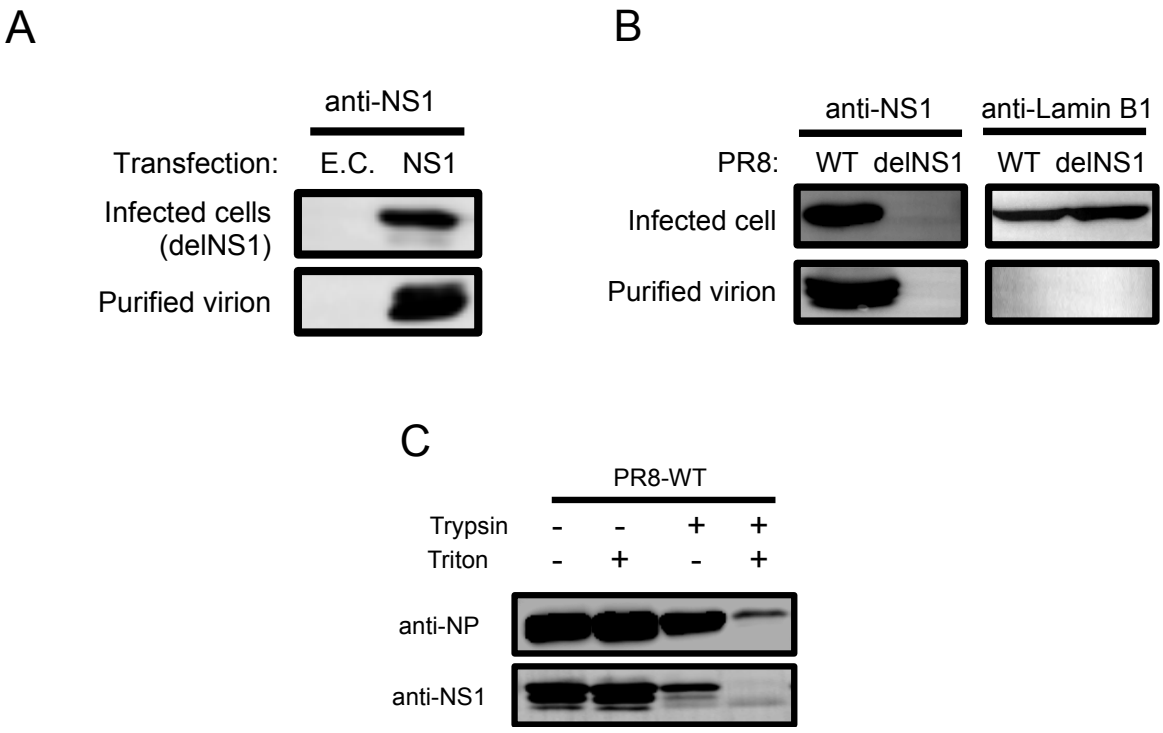

Fig 3.5 Detection of NS1 in virus particle

(A) Virus particle purified from Fig 3.4-A and (B) MDCK cells infected with either PR8-WT or PR8-delNS1 were subject to SDS-PAGE and protein amount was determined using anti-NS1 and anti-Lamin B antibodies. (C) Virus particle purified from PR8-WT infected MDCK cells were treated with either triton or trypsin or both and subject SDS-PAGE. Protein amount was determined using anti-NP and anti-NS1 antibodies.

3.6 NS1 increases viral genome packaging efficiency.

Fig 3.4-B showed that level of NP in purified virus fraction was significantly higher in NS1 expressing cells. However, it is not clear that whether the increase is simply due to the presence of higher amounts of virus particle or higher packaging efficiency of genomic viral RNA associated NP (RNP). To clarify this, genomic viral RNA was extracted from the same HAU of virus particles from E.C. and NS1 expressing cells. RT-qPCR revealed that the relative amounts of segments 4-8 were significantly enhanced in virus fraction from NS expressing cells (Fig 3.6-A). The difference was more dramatic in segment 5 and 6. To directly visualise the genomic viral RNA in the presence or absence of NS1, genomic viral RNA was extracted from PR8-WT and PR8-delNS1 infected MDCK cells and resolved by Urea-PAGE. Given that the same amount of RNA was applied (200ng), PR8-delNS1 virus exhibited less RNA quantity for all segments than PR8-WT virus and with more significant difference for segment 5-8 (Fig 3.6-B). RNA sample of segment 8 (NS, 418 bases) from PR8-delNS1 was only barely detected. Interestingly, both PR8-WT and PR8-delNS1 contained the most abundant amount of RNA corresponding to segment 4 (HA, 1775 bases), suggesting the packaging efficiency of segment 4 is the highest among all eight segments (Fig 3.6-C).

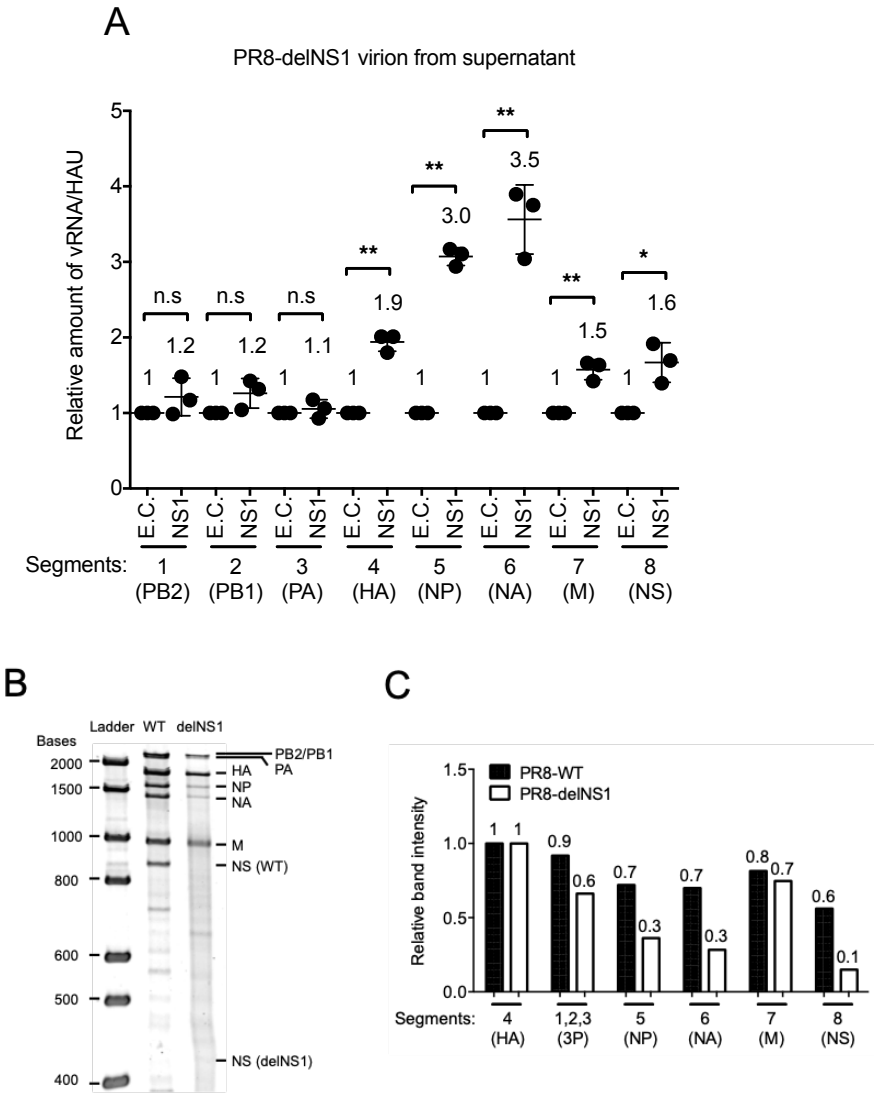

Fig 3.6 Effect of NS1 on viral genome packaging

(A) vRNA extracted from equal HAU of virus from E.C. and NS1 expressing cells from Fig. 3.4-A were subjected to RT-qPCR quantification. Levels of viral genome from E.C. transfected cells were set to 1. The data shown are the mean ± standard deviation from at least three independent experiments (n=3). The Student's t test was used for statistical analysis (n.s. not significant, *P<0.05, **P<0.01). (B) Equal amount (200 ng) of vRNA extracted from PR8-WT or PR8-delNS1 infected MDCK cells were subjected to Urea-PAGE. Viral genomic RNA segments were directly visualised under UV irradiation. (C) The band intensity of individual segments was determined from (B). Relative band intensity of individual segments was expressed as band intensity relative to segment 4 (HA). Relative band intensity of segment 4 (HA) was set to 1.

3.7 Viral genomic RNA replication is not affected by NS1.

To examine whether the enhancement of genome packaging in the presence of NS1 correlates to the level of viral genomic RNA in infected cells, total RNA was extracted from infected cells in the presence or absence of exogenous NS1 expression. RT-qPCR using primers targeting viral genomic RNA revealed that NS1 has no significant effect on viral genomic RNA replication in segment 1-3, 7 and 8 (Fig 3.7-A). Although a significant increase in segment 4-6 was detected in cells expressing NS1, the differences were less than 2-fold (Fig 3.7-A). Moreover, a virus like particle based minigenome assay was employed to examine the effect of NS1 on IAV RNA dependent RNA polymerase (RdRP) activity. In this assay, an RNA polymerase I (pol I) based IAV minigenome plasmid, which encodes a luciferase reporter, was co-expressed with a total of 9 viral protein in HEK 293T RIG-I KO cells (donor cells) in the presence or absence of exogenous NS1 expression (Fig 3.7-B). Luciferase quantification of transfected cell lysate indicated that NS1 has no significant effect on luciferase minigenome expression and replication (Fig 3.7-C). Quantification of minigenome viral RNA in transfected cells also showed a similar result (Fig 3.7-D). The luciferase minigenome was constructed based on the untranslated region (UTR) derived from segment 8. A segment 5 UTR derived luciferase minigenome was also generated and analysed. Similarly, NS1 has no significant effect on segment 5 based luciferase minigenome expression in transfected cells (Fig 3.7-E). Taken together, replication of viral genomic RNA is unchanged regardless the presence or absence of NS1.

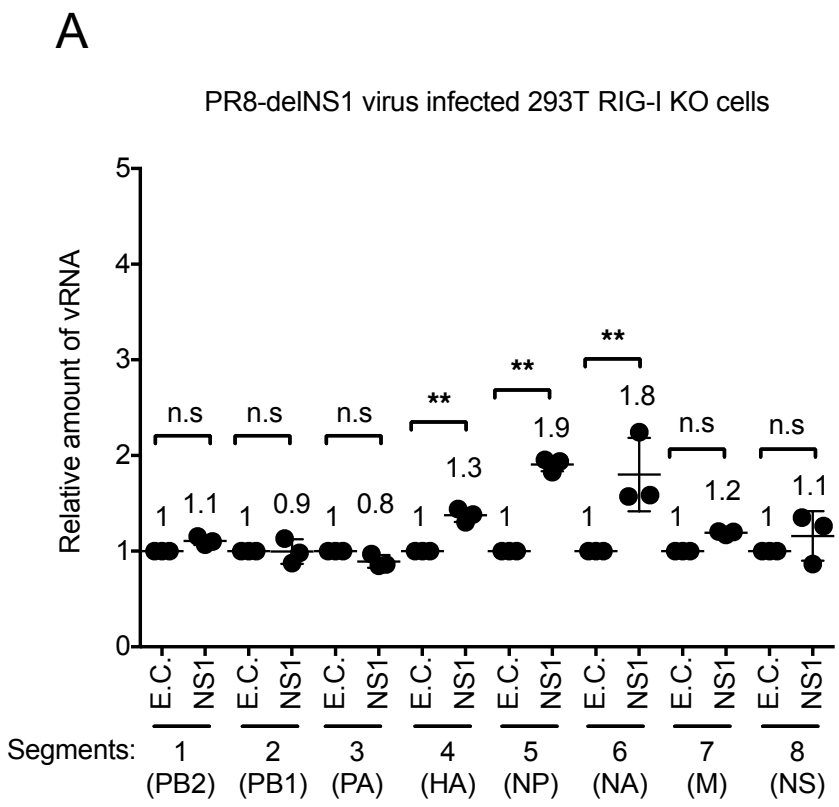

Fig 3.7 Effect of NS1 on viral genome replication

(A) Total RNA from infected cells from Fig. 3.4-A were extracted and quantified by RT-qPCR using primer targeting vRNA of individual segment. Levels of viral genome obtained from E.C. transfected cells were set to 1. The data shown are the mean ± standard deviation from at least three independent experiments (n=3). The Student's t test was used for statistical analysis (n.s. not significant, *P<0.05, **P<0.01).

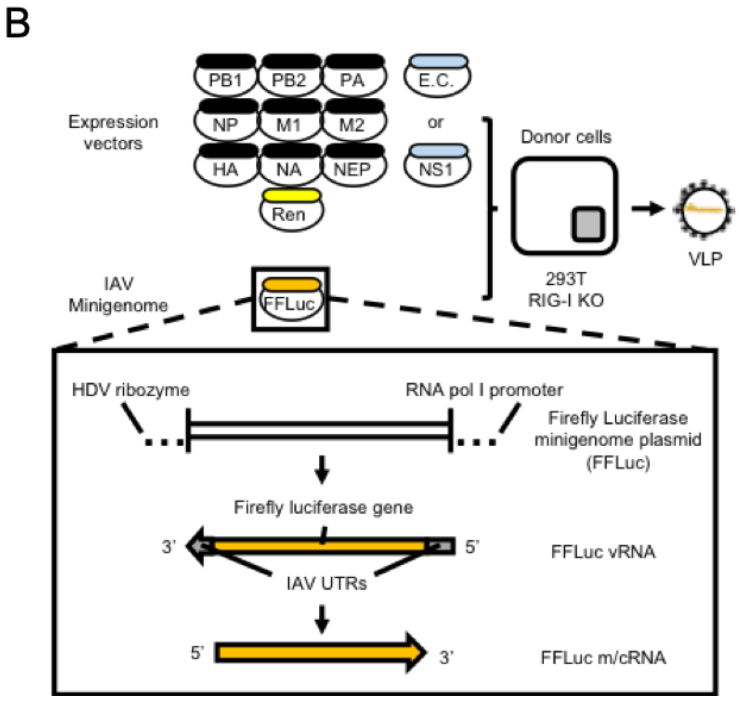

Fig 3.7 Effect of NS1 on viral genome replication

(B) 293T RIG-I KO cells (donor cells) were co-transfected with eleven expression plasmids as described (Materials and Methods) and a minigenome expression construct. The negative sense minigenome vRNA is synthesised by RNA pol I as illustrated and replicated by IAV RdRP (PB2, PB1 and PA).

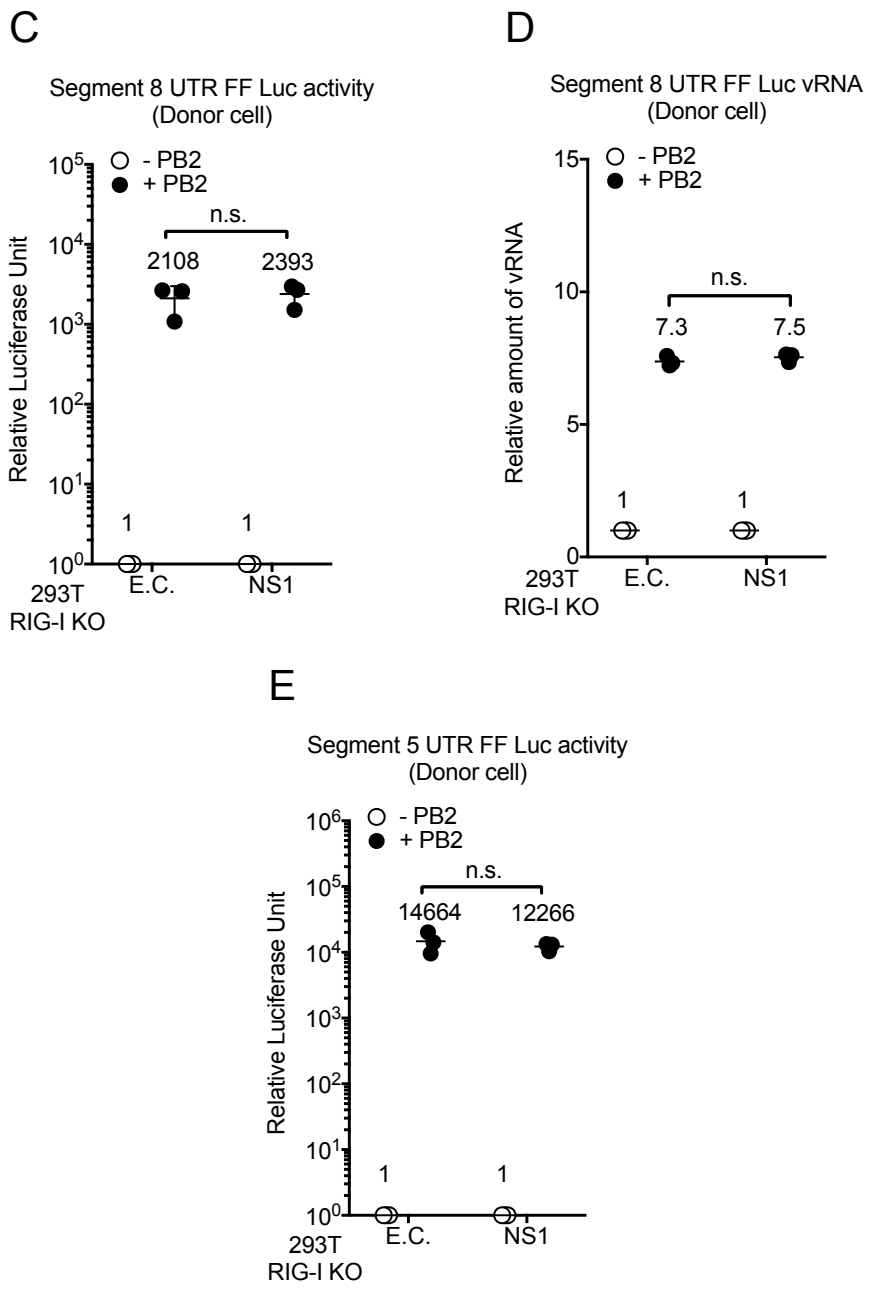

Fig 3.7 Effect of NS1 on viral genome replication

Donor cells from (B) were analysed for Luciferase expression (C and E) or Luciferase vRNA quantity (D) after 48 hours post transfection. Firefly luciferase activity was normalised to Renilla luciferase activity. Luciferase activity or vRNA quantity of cells without PB1 expression was set to 1. The one-way ANOVA followed by Tukey's test was used for statistical analysis (n.s. not significant). The data shown are the mean ± standard deviation from at least three independent experiments (n=3).

3.8 NS1 enhances luciferase minigenome packaging in VLP production system.

Fig 3.6-A showed that NS1 increases genome packaging efficiency of segments 4-8 in the virus infection setting. This phenotype was also analysed in the VLP production system. Supernatant was collected from co-transfected cells in Fig 3.7-B in the presence or absence of NS1 and inoculated to either HEK 293T WT or RIG-I KO cells (Recipient cells), which were pre-transfected with IAV RdRP and NP (Fig 3.8-A). After 8 hours post VLP infection, luciferase activity of recipient cells was measured. Interestingly, recipient cells infected with VLP generated from NS1 expressing donor cells exhibited significantly increased luciferase activity (Fig 3.8-B). A similar result was observed in a segment 5 UTR based luciferase reporter VLP infection (Fig 3.8-C). In addition to luciferase expression quantification, immunofluorescence microscopy using an anti-luciferase antibody also showed that the number of recipient cells infected with VLP generated from NS1 expressing donor cells was significantly higher (Fig 3.8-D).

It is not clear that whether the increased incidence of infected recipient cells and hence the higher luciferase signal is due to enhancement of minigenome packaging into VLP or simply because of higher titre of VLP that is generated in NS1 expressing donor cells. Therefore, determination of VLP titre is necessary. VLP in supernatant from donor cells in the presence or absence of NS1 was concentrated and purified. Then, the same volume of VLP fractions were resolved by SDS-PAGE. Western blot data revealed that the levels of M1 and HA2 in the VLP fraction were unaffected regardless the presence or absence of NS1 in donor cells (Fig 3.8-E, Purified VLP). In contrast, the VLP fraction from NS1 expressing donor cells showed a higher NP level (Fig 3.8-E, Purified VLP). Moreover, NS1 was also detected in the

VLP fraction (Fig 3.8-E, Purified VLP). The level of viral protein was also analysed in donor cells. Both NP, M1 and HA2 levels were unaffected regardless of the presence or absence of NS1 (Fig 3.8-E, Donor cells). RNA was purified from VLP fractions and subjected to RT-qPCR analysis. Given that the amount of VLP produced in donor cells was the same regardless of the presence or absence of NS1, VLP from NS1 expressing donor cells showed a significantly higher amount of viral minigenome reporter RNA than those produced from control expressing donor cells (Fig 3.8-F). Taken together, the VLP production system shows that NS1 is important for enhancing viral genomic RNA packaging efficiency.

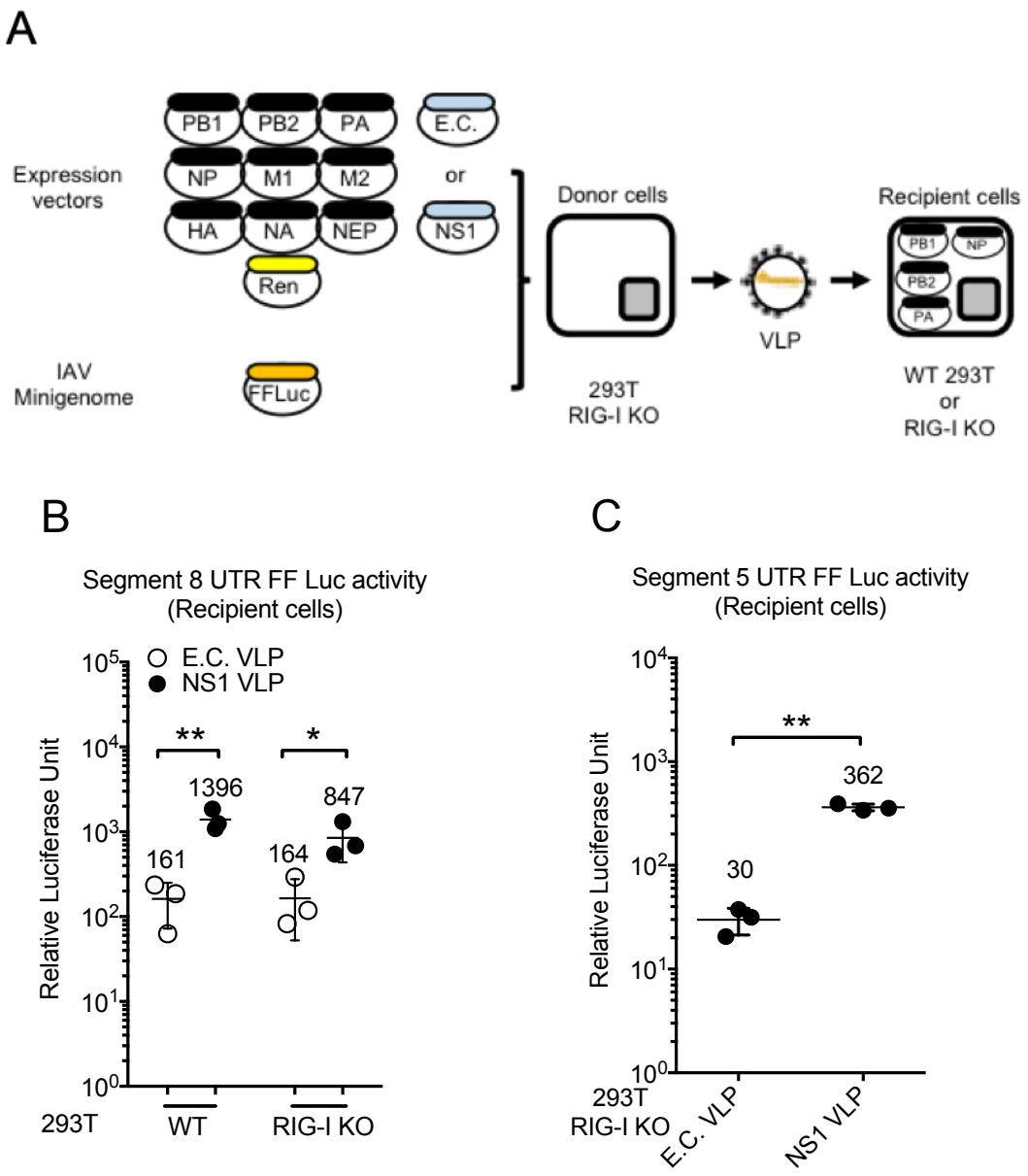

Fig 3.8 Effect of NS1 on minigenome packaging into VLP

(A) VLP collected from donor cells from Fig 3.7-B was treated with benzonase nuclease and added to recipient cells (HEK 293T WT or RIG-I KO) which are pre-transfected with pCAGGS-PB2, PB1 and PA (Materials and Methods). (B and C) Luciferase activity of recipient cells were measured after 8 hours post VLP infection. The data shown are the mean ± standard deviation from at least three independent experiments (n=3). The Student's t test was used for statistical analysis (*P<0.05, **P<0.01).

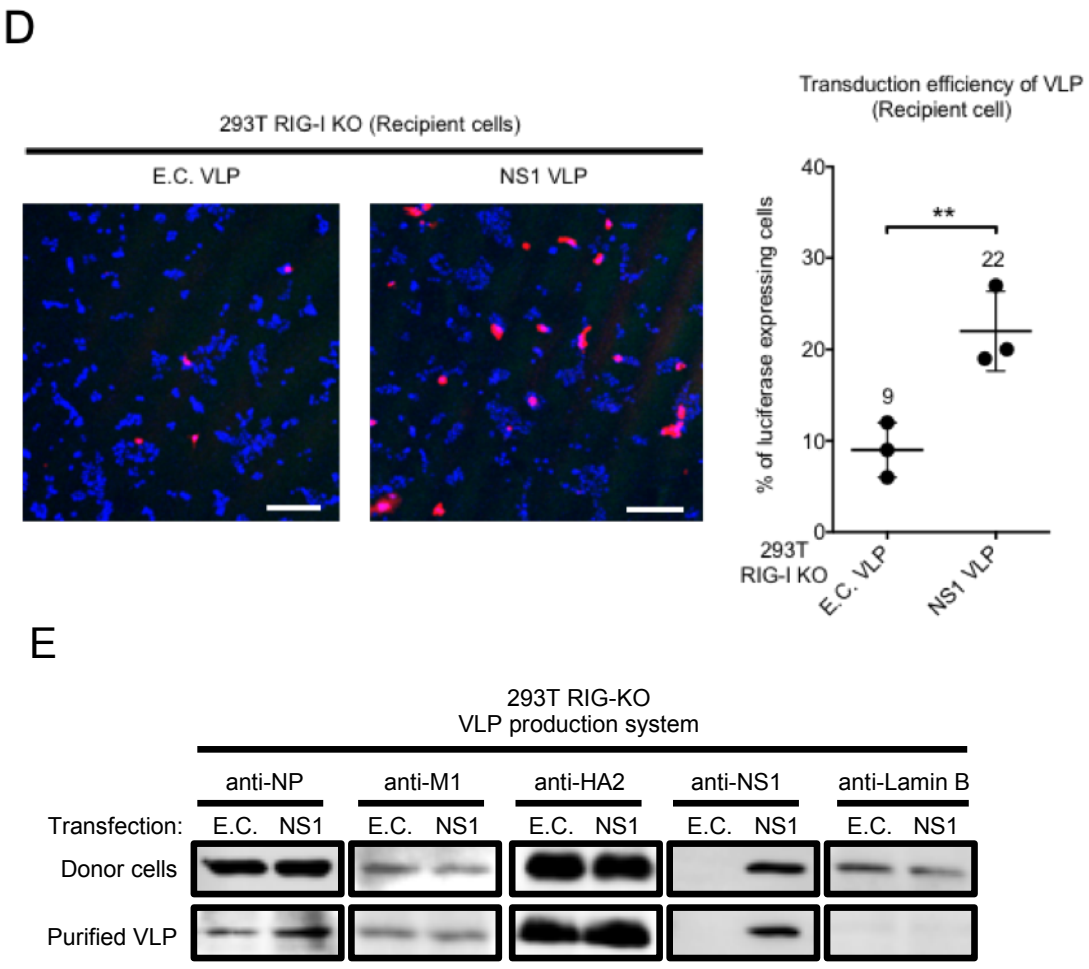

Fig 3.8 Effect of NS1 on minigenome packaging into VLP

(D) VLP infected recipient cells (HEK 293T RIG-I KO) were stained with anti-luciferase antibody (Red) and DAPI (Blue), and examined by confocal microscopy (left) after 24 hours post infection. Scale bar, 10μm. Positive cells (Red) were quantified for luciferase expression (right). The data shown are the mean ± standard deviation from at least three independent experiments (n=3). The Student's t test was used for statistical analysis (**P<0.01). (E) Donor cells lysate and purified VLP from Fig 3.7-B were subjected to SDS-PAGE. Protein amount was determined using anti-NP, anti-M1, anti-HA2 (cleaved HA) and anti-Lamin B antibodies.

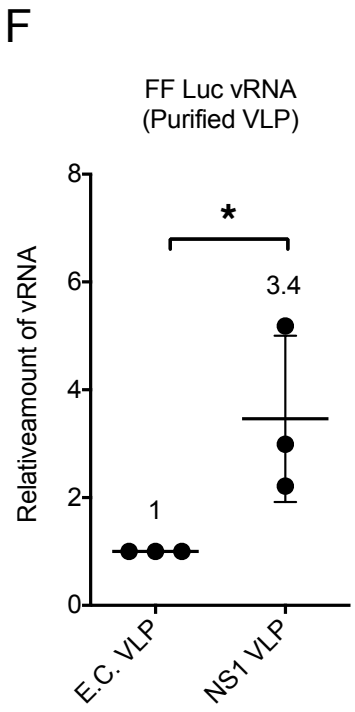

Fig 3.8 Effect of NS1 on minigenome packaging into VLP

(F) vRNA was extracted from equal volume of purified VLP suspension (E.C. vs. NS1) and quantified by RT-qPCR using primer set targeting luciferase gene. The data shown are the mean ± standard deviation from at least three independent experiments (n=3). The Student's t test was used for statistical analysis (*P<0.05).

3.9 Double-stranded RNA (dsRNA) binding domain of NS1 is involved in virus production.

NS1 consists of a dsRNA binding domain, an effector domain and a tail domain (Fig 3.9-A). The dsRNA binding domain was reported to be critical in multiple functions of NS1 including RIG-I antagonism [7, 13, 15, 32, 33]. Therefore, the effect of dsRNA binding domain on virus production was investigated. R38A point mutation, a classical NS1 dsRNA binding domain mutant, was introduced to the expression plasmid which encodes NS1 WT. HEK 293T RIG-I KO cells were infected with PR8-delNS1 virus and subsequently transfected with an E.C. or NS1 R38A expression plasmid. Same volumes of virus fraction was prepared from supernatant and the level of viral structural proteins (NP, M1 and HA) were determined by Western blot. The level of viral structural proteins in virus fraction from NS1 R38A expressing cells was decreased and the largest difference was observed in M1 and HA2 protein levels (Fig 3.9-B, Purified virion). The level of M1 and HA2 protein in NS1 R38A expressing cells infected with PR8-delNS1 virus exhibited a similar pattern as in virus fractions (Fig 3.9-B, Infected cells). Strikingly, although expression levels of NS1 R38A were similar to NS1 WT in virus-infected cells, the incorporation of NS1 R38A into virus particle was severely impaired (Fig 3.9-B, Purified virus). HA assay revealed that virus production from NS1 R38A expressing cells was reduced by approximately 2-fold (Fig 3.9-C). Moreover, plaque assay showed that NS1 R38A expressing cells produced less infectious viruses and the virus titre was comparable to E.C. expressing cells (Fig 3.9-D). These results suggested that disruption of dsRNA binding domain in NS1 reduces virus production and infectivity.

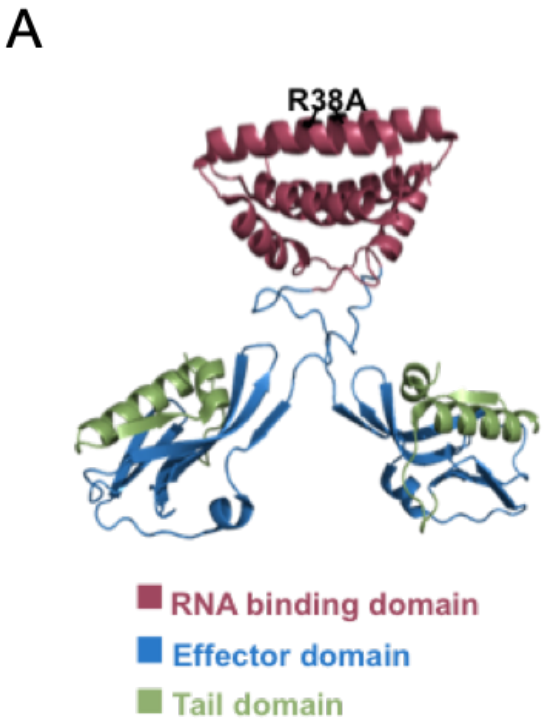

Fig 3.9 Involvement of NS1 dsRNA binding domain on virus production and infectivity

(A) Schematic representation of NS1 dimer showing RNA binding domain (Red), effector domain (Blue) and Tail domain (Green).

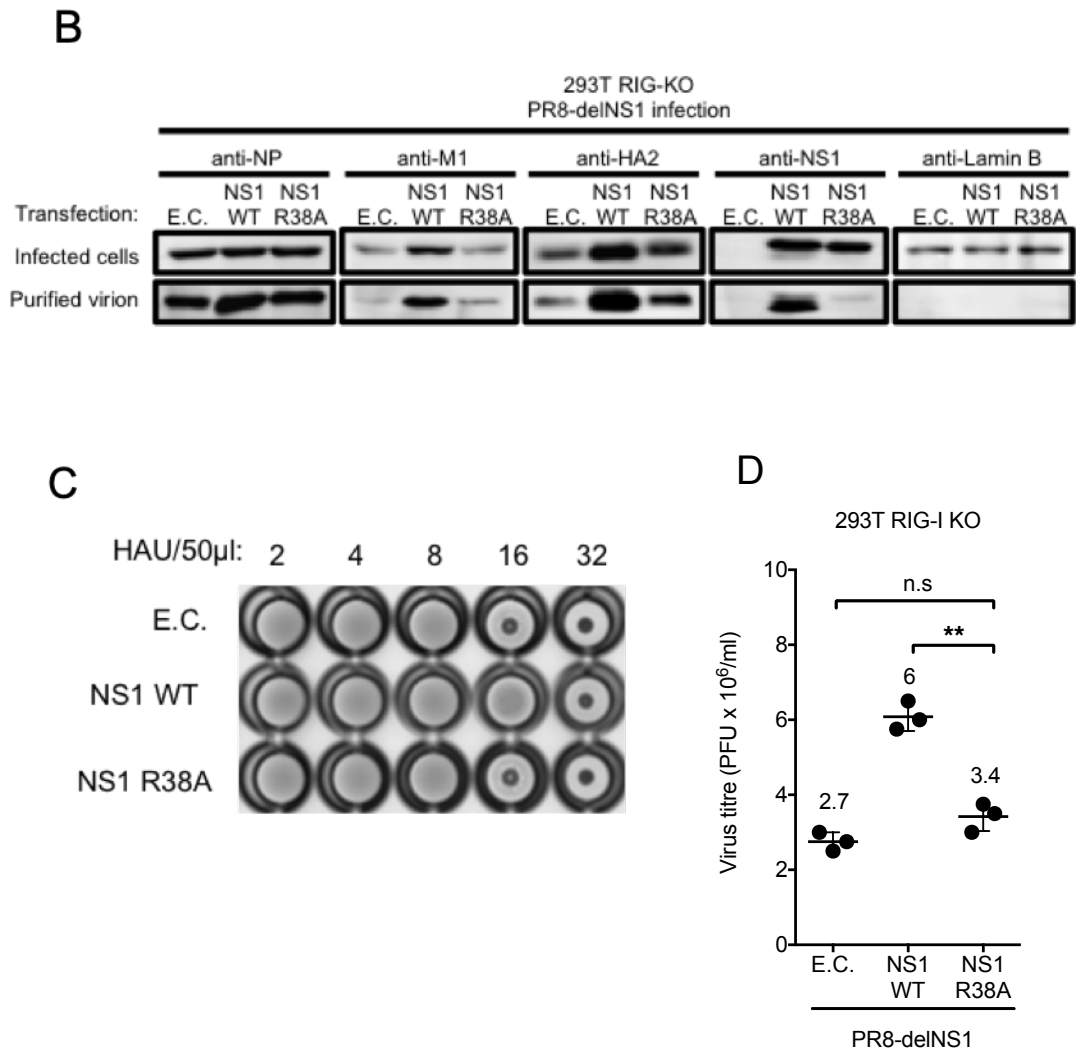

Fig 3.9 Involvement of NS1 dsRNA binding domain on virus production and infectivity

(B) HEK 293T RIG-I KO cells were infected with PR8-delNS1 at MOI 0.01 and transfected with empty vector (E.C.), pEF-Bos-NS1 WT or NS1 R38A as shown in Fig 3.4-A. Cell lysate and purified virion were subjected to SDS-PAGE. Protein amount was determined using anti-NP, anti-M1, anti-HA2 (cleaved HA) and anti-Lamin B antibodies. (C) Virus titre (HAU/50µl) was determined from supernatant collected from (B) using HA assay. (D) Infectious virus titre (PFU/ml) was determined by plaque assay using MDCK cells. The data shown are the mean ± standard deviation from at least three independent experiments (n=3). The one-way ANOVA followed by Tukey's test was used for statistical analysis (n.s. not significant **P<0.01).

3.10 DsRNA-binding domain of NS1 is involved in viral genomic RNA packaging.

The effect of dsRNA-binding domain on viral genomic RNA packaging was also investigated. Supernatant was collected from HEK 293T RIG-I KO donor cell, which were co-transfected with plasmids for VLP production as in Fig 3.7-B, together with E.C., NS1 WT or NS1 R38A expression. Supernatant from donor cells was inoculated to HEK 293T RIG-I KO recipient cells, which were pre-transfected with IAV RdRP and NP. Luciferase expression was partially reduced in recipient cells infected with VLP generated from NS1 R38A expressing donor cells (Fig 3.10-A). RNA level from purified VLP fraction was also determined by RT-qPCR. A significant reduction of viral genomic RNA was observed in VLP fraction from NS1 R38A expressing cells (Fig 3.10-B). Moreover, the amount of viral structural protein in VLP was also analysed by SDS-PAGE. No significant effect on viral protein amount in purified VLP fraction from NS1 R38 expressing donor cells indicated that VLP titre was unaffected by NS1 R38A (Fig 3.10-C, Purified VLP). Similarly, NS1 R38A expression in donor cells exhibited no effect on viral protein expression (Fig 3.10-C, Donor cells). Interestingly, the incorporation of NS1 R38A into VLP was severely reduced (Purified VLP). These results suggested that dsRNA binding domain of NS1 is involved in viral genomic RNA packaging.

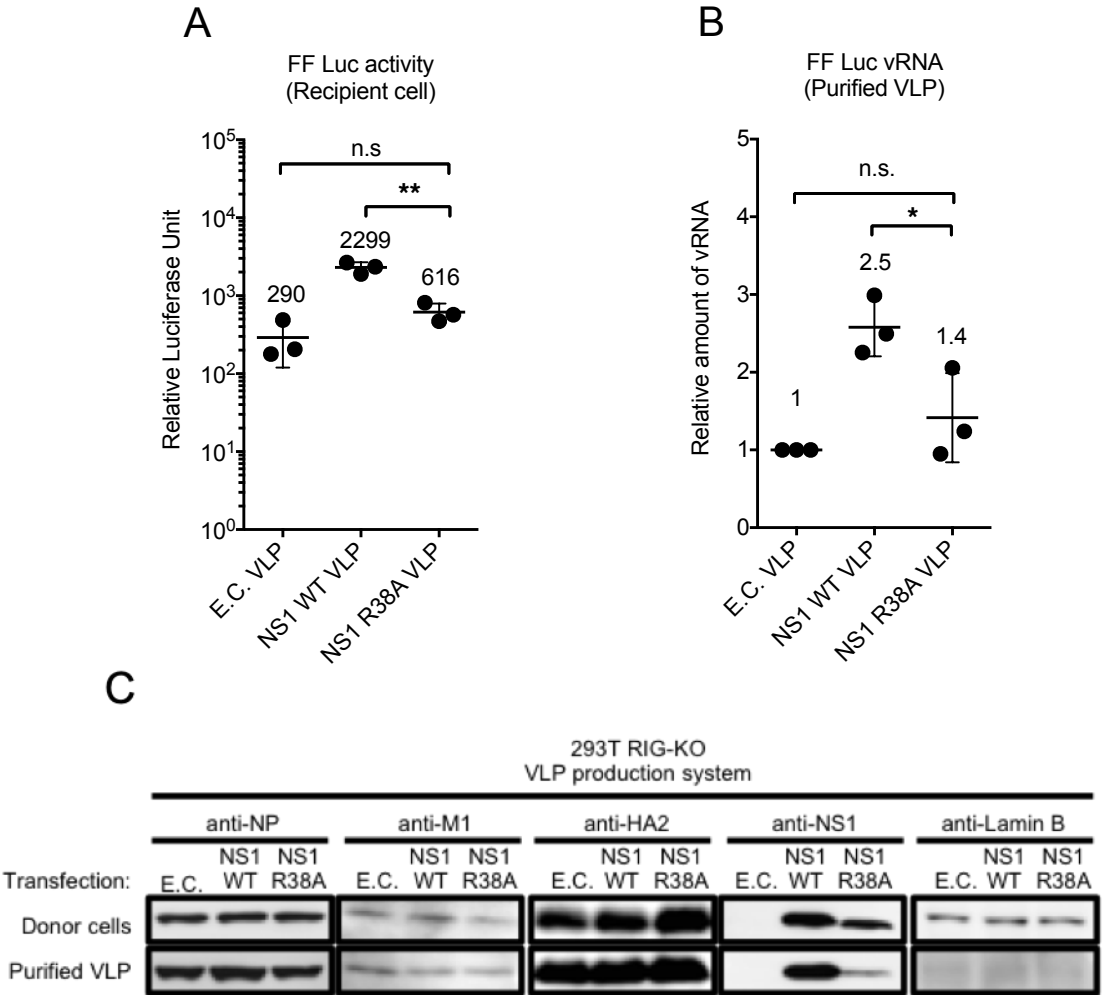

Fig 3.10 Involvement of NS1 dsRNA binding domain on minigenome packaging in VLP

(A) VLP collected from donor cells expressing E.C., NS1 WT or NS1 R38A were treated with benzonase nuclease and added to recipient cells (HEK 293T RIG-I KO) which are pre-transfected with pCAGGS-PB2, PB1 and PA (Materials and Methods). Luciferase activity of recipient cells were measured after 8 hours post VLP infection. The data shown are the mean ± standard deviation from at least three independent experiments (n=3). The one-way ANOVA followed by Tukey's test was used for statistical analysis (n.s. not significant *P<0.05, **P<0.01). (B) vRNA was extracted from an equal volume of purified VLP suspension (E.C. vs. NS1 WT vs. NS1 R38A) and quantified by RT-qPCR using primer set targeting luciferase gene. The data shown are the mean ± standard deviation from at least three independent experiments (n=3). The one-way ANOVA followed by Tukey's test was used for statistical analysis (*P<0.05). (C) Donor cells lysate and purified VLP were subjected to SDS-PAGE. Protein amount was determined. Protein amount was determined using anti-NP, anti-M1, anti-HA2 (cleaved HA) and anti-Lamin B antibodies.

Chapter 4

Discussion

The function of NS1 to antagonise RIG-I antiviral response has been studied extensively. However, other functions which are intrinsically related to virus life cycle and replication was remained elusive. In this report, the NS1 functions which are independent of its role on RIG-I and IFN-I antiviral signalling antagonism was investigated and characterised.

The delNS1 virus is a useful tool to study the function of NS1. PR8-delNS1 infection of HEK 293T WT cells induced robust IFN-I level (Fig 3.1-A) and replicate inefficiently in WT cells (Fig 3.1-B). Due to the lack of NS1 protein, delNS1 virus is sensed by a cytoplasmic RNA sensor RIG-I and induce strong antiviral response during replication. Previous study showed that the attenuation of PR8-delNS1 can be rescued in innate immunity incompetent cells such as Vero cells, in which the IFN-I gene is absent, hence confirms the role of NS1 in antagonising IFN-I antiviral response. However, a full rescue of PR8-delNS1 in Vero cells is not achieved [34]. Similarly, infection of HEK 293T RIG-I KO cells, which a cell line lacking RIG-I signal transduction, with PR8-delNS1 fails to produce a similar titre as in PR8-WT infection (Fig 3.1-C). Sanger sequencing of full viral genome reveals multiple nucleotide differences between PR8-WT and PR8-delNS1 (Table 3), as a result of spontaneous mutation during propagation of these viruses. These differences could result in a different rate of replication and gene expression. However, in a series of experiments using plasmid driven NS1 expression, virus titre of PR8-delNS1 can be further enhanced if NS1 is present in RIG-I KO cells (Fig 3.4-A). Similar results were observed in a luciferase reporter minigenome-based VLP production system that exogenous NS1 expression in RIG-I KO cells enhances the infectivity of VLP (Fig. 3.8-B-D). These results indicate that NS1 is required to optimise the virus titre and infectivity, independent of RIG-I antiviral signalling antagonism.

To investigate how NS1 optimises infectivity, the effect of NS1 on viral protein expression amount was examined. Western blot of infected cell lysate revealed that viral structural protein M1 and HA expression of PR8-delNS1 was enhanced in NS1 expressing cells (Fig 3.4-B). The precise mechanisms of this enhancement need further investigation. Previous studies showed that NS1 promote viral mRNA nuclear export, which could result in enhanced accumulation of viral protein in infected cells [35, 36]. Interestingly, NP level is unaffected regardless the presence or absence of NS1. Marion et al and Hatada et al demonstrated that the untranslated region between each segment are different and NS1 binds specifically to these regions [37, 38]. Therefore, NS1 could control viral gene expression and translation in a segment specific manner. Although NS1 alters expression of viral structural protein, it has no significant effect on respective level of viral genomic RNA (Fig 3.7). This suggests that effect of NS1 is acting on viral gene expression rather than viral genome replication. There is a strong correlation between M1 and HA level in cells and virus production (Fig 3.4-B and 3.4-D). The up-regulated expression of HA protein on the cell surface may stimulate the budding process and hence produce more virus particles [39]. However, VLP production system data showed that VLP production is not affected by NS1 because M1 and HA expression remains unchanged (Fig 3.8-D). This discrepancy is possibly due to different expression mechanisms of viral proteins between virus and VLP. In virus, different viral mRNAs are transcribed by viral RdRP whereas in VLP, the viral proteins are expressed from plasmids and transcribed by cellular RNA polymerase II. Also, only the open reading frame but not the full genome with UTR is included in expression plasmids of a viral gene. Therefore, NS1 is not able to regulate plasmid based viral gene expression.

Quantification of viral genomic RNA in supernatant showed that NS1-expressing cells produce virus containing higher amounts of viral gene segments than NS1 non-expressing cells (Fig 3.6). Also, VLP production system data revealed that VLP produced from NS1 expressing cells generally incorporate a higher amount of reporter viral genomic RNA and hence higher transduction efficiency (Fig 3.8-B, C and F). These results suggest that a second role of NS1 is to enhance viral genomic RNA packaging. However, the exact mechanism of NS1-mediated genome packaging requires further investigation. Previously, Fodor et al showed that NS1 interacts with NP, which is associated with viral genomic RNA to form viral RNP complex [40]. Furthermore, a NS1 interactome analysis in host cells revealed that NS1 also binds KIF11, a motor protein that moves along cellular microtubule [41]. Therefore, NS1 could facilitate the RNP complex transportation mediated by microtubule [42]. Thus it is interesting to speculate that NS1 enhances packaging efficiency of the viral RNP into a virus particle through regulation of dynamic intracellular logistics (Fig. 4). Because IAV is a segmented virus, it requires a complete set of 8 segments to initiate successive replication cycle. Enhancement of genome packaging efficiency by NS1 could potentially increase the chance for generating virus particle with a complete set of segments, thus enhancing infectivity. Interestingly, some specificities on NS1-mediated genome packaging are observed. NS1 preferably enhance segment 5, 6 and 8 (Fig. 3.6 A and C). This is supported with VLP production system that NS1 enhances the transduction of VLP containing luciferase reporter flaked by segment 5 or 8 UTR. By recognising the specific UTR sequence of a viral genomic RNA, NS1 can selectively enhance the packaging of these segments [38]. However, how exactly NS1 achieves this specificity and

whether NS1 directly interacts with these viral genomic segments requires further investigation.

Protein analysis of PR8-delNS1 virus particles produced from NS1 expressing cells or PR8-WT virus showed that NS1 is incorporated into the virus particle. (Fig 3.5-A and B). Furthermore, NS1 is also pre-packaged in VLP produced from NS1 expressing cells. These results are in line with a previous study which unambiguously detect NS1 in purified virus particle in the WSN strain [21]. NS1 could serve as an adaptor protein, which facilitates the eight-segment arrangement in IAV particles. However, it is unclear that whether NS1 incorporation is spontaneous or intentional. In fact, STAUFEN1, a host cell dsRNA binding protein , has been shown to be incorporated into HIV particles and enhance packaging of the HIV genome [43]. The direct correlation of NS1 mediated viral genome packaging and incorporation of NS1 needs further investigation.

The involvement of RNA binding domain of NS1 was also investigated. Mutation of the RNA-binding domain (R38A) of NS1 failed to elevate virus titre and VLP infectivity (Fig 3.9-D and 3.10-A). In line with this, levels of M1 and HA expression clearly reduced in NS1 R38A-expressing cells, which results in reduction of virus production (Fig 3.9-B and 3.9-C). The NS1 dsRNA-binding domain could play a role in recognising the UTR region of viral genomic RNA. However, detailed mechanisms of this recognition require further investigation. Moreover, genome packaging efficiency is also greatly reduced in VLP produced from NS1 R38A-expressing cells (Fig. 3.10-B). These results suggest that the RNA-binding domain of NS1 is involved in optimising virus infectivity through enhancing both virus production and genome packaging. Of note, incorporation of NS1 R38A into the virus particle and VLP is severely impaired, suggesting NS1 incorporation is also dsRNA-

binding dependent. However, whether NS1 dsRNA-binding domain directly interacts with viral genomic RNA within virus particle is not clear.

In summary, this study puts forth evidence for new roles of NS1 in virus production and viral genome packaging which optimise IAV infectivity. Furthermore, dsRNA-binding domain of NS1 is important for these functions. Thus, targeting dsRNA binding domain of NS1 is an attractive approach to develop antiviral compounds against IAV infection.

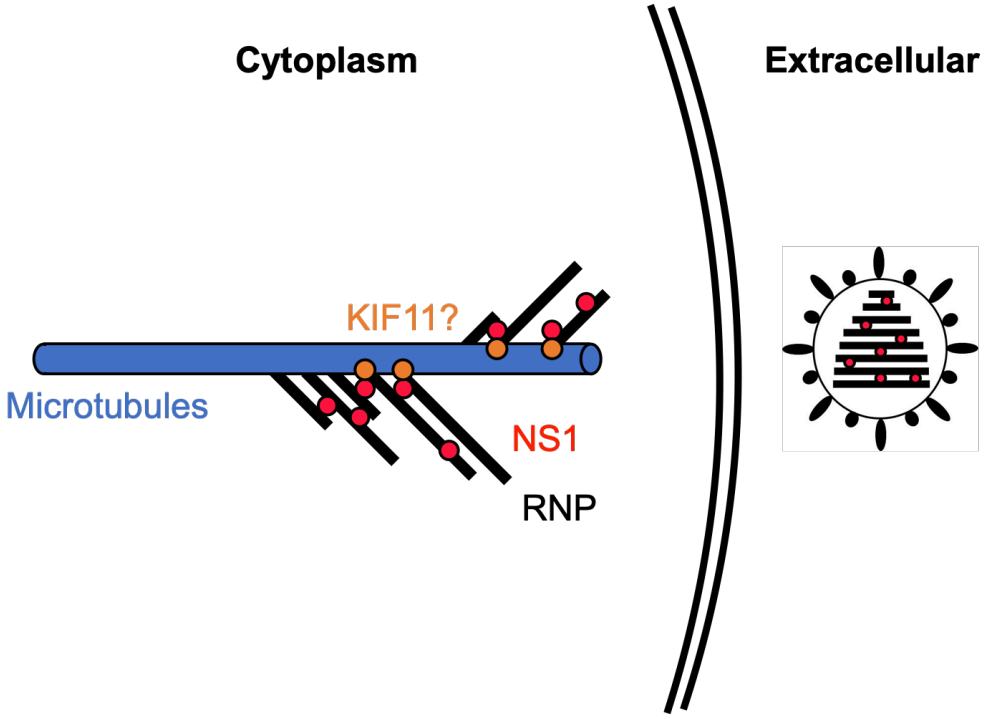

Fig 4. Schematic representation of proposed model of NS1-mediated RNP packaging.

Prior to virus budding, influenza RNP segments travel along microtubules in host cells through a Rab11 dependent mechanism. NS1 interacts with different RNP segments and thereby optimises for eight segments packaging. It is hypothesised that NS1 also interacts with a microtubule associated motor protein KIF11 and thereby regulating the microtubule dynamics, which is crucial for Rab11 mediated transport of RNP segments. The interaction of NS1 with microtubule components could also enhance viral genome packaging in IAV.

Chapter 5

Bibliography

References

1. Taubenberger JK, Morens DM: **1918 Influenza: the mother of all pandemics.** Emerg Infect Dis 2006, **12**(1):15-22.

2. Noda T, Sagara H, Yen A, Takada A, Kida H, Cheng RH, Kawaoka Y: **Architecture of ribonucleoprotein complexes in influenza A virus particles.** Nature 2006, **439**(7075):490-492.

3. Arranz R, Coloma R, Chichón FJ, Conesa JJ, Carrascosa JL, Valpuesta JM, Ortín J, Martín-Benito J: **The structure of native influenza virion ribonucleoproteins.** Science 2012, **338**(6114):1634-1637.

4. Sun X, Whittaker GR: **Entry of influenza virus.** Adv Exp Med Biol 2013, **790**:72-82.

5. Dou D, Revol R, Östbye H, Wang H, Daniels R: **Influenza A Virus Cell Entry, Replication, Virion Assembly and Movement.** Front Immunol 2018, **9**:1581.

6. Hale BG, Randall RE, Ortín J, Jackson D: **The multifunctional NS1 protein of influenza A viruses.** J Gen Virol 2008, **89**(Pt 10):2359-2376.

7. Yoneyama M, Kikuchi M, Natsukawa T, Shinobu N, Imaizumi T, Miyagishi M, Taira K, Akira S, Fujita T: **The RNA helicase RIG-I has an essential function in double-stranded RNA-induced innate antiviral responses.** Nat Immunol 2004, **5**(7):730-737.

8. Jureka AS, Kleinpeter AB, Tipper JL, Harrod KS, Petit CM: **The influenza NS1 protein modulates RIG-I activation via a strain-specific direct interaction with the second CARD of RIG-I.** J Biol Chem 2020, **295**(4):1153-1164.

9. Jureka AS, Kleinpeter AB, Cornilescu G, Cornilescu CC, Petit CM: **Structural Basis for a Novel Interaction between the NS1 Protein Derived from the 1918 Influenza Virus and RIG-I.** Structure 2015, **23**(11):2001-2010.

10. Koliopoulos MG, Lethier M, van der Veen, A. G., Haubrich K, Hennig J, Kowalinski E, Stevens RV, Martin SR, Reis E Sousa C, Cusack S, Rittinger K: **Molecular mechanism of influenza A NS1-mediated TRIM25 recognition and inhibition.** Nat Commun 2018, **9**(1):1820-8.

11. Moriyama M, Chen IY, Kawaguchi A, Koshiba T, Nagata K, Takeyama H, Hasegawa H, Ichinohe T: **The RNA- and TRIM25-Binding Domains of Influenza Virus NS1 Protein Are Essential for Suppression of NLRP3 Inflammasome-Mediated Interleukin-1beta Secretion.** J Virol 2016, **90**(8):4105-4114.

12. Salvatore M, Basler CF, Parisien JP, Horvath CM, Bourmakina S, Zheng H, Muster T, Palese P, Garcia-Sastre A: **Effects of influenza A virus NS1 protein on protein expression: the NS1 protein enhances translation and is not required for shutoff of host protein synthesis.** J Virol 2002, **76**(3):1206-1212.

13. Min JY, Li S, Sen GC, Krug RM: **A site on the influenza A virus NS1 protein mediates both inhibition of PKR activation and temporal regulation of viral RNA synthesis.** Virology 2007, **363**(1):236-243.

14. Schierhorn KL, Jolmes F, Bespalowa J, Saenger S, Peteranderl C, Dzieciolowski J, Mielke M, Budt M, Pleschka S, Herrmann A, Herold S, Wolff T: **Influenza A Virus Virulence Depends on Two Amino Acids in the N-Terminal Domain of Its NS1**

Protein To Facilitate Inhibition of the RNA-Dependent Protein Kinase PKR. J Virol 2017, **91**(10):10.1128/JVI.00198-17. Print 2017 May 15.

15. Li S, Min JY, Krug RM, Sen GC: **Binding of the influenza A virus NS1 protein to PKR mediates the inhibition of its activation by either PACT or double-stranded RNA.** Virology 2006, **349**(1):13-21.

16. Ehrhardt C, Wolff T, Pleschka S, Planz O, Beermann W, Bode JG, Schmolke M, Ludwig S: **Influenza A virus NS1 protein activates the PI3K/Akt pathway to mediate antiapoptotic signaling responses.** J Virol 2007, **81**(7):3058-3067.

17. Falcón AM, Fortes P, Marión RM, Beloso A, Ortín J: **Interaction of influenza virus NS1 protein and the human homologue of Staufen in vivo and in vitro.** Nucleic Acids Res 1999, **27**(11):2241-2247.

18. de la Luna S, Fortes P, Beloso A, Ortin J: **Influenza virus NS1 protein enhances the rate of translation initiation of viral mRNAs.** J Virol 1995, **69**(4):2427-2433.

19. Park YW, Katze MG: **Translational control by influenza virus. Identification of cis-acting sequences and trans-acting factors which may regulate selective viral mRNA translation.** J Biol Chem 1995, **270**(47):28433-28439.

20. Enami K, Sato TA, Nakada S, Enami M: **Influenza virus NS1 protein stimulates translation of the M1 protein.** J Virol 1994, **68**(3):1432-1437.

21. Hutchinson EC, Charles PD, Hester SS, Thomas B, Trudgian D, Martinez-Alonso M, Fodor E: **Conserved and host-specific features of influenza virion architecture.** Nat Commun 2014, **5**:4816.

22. Weber M, Sediri H, Felgenhauer U, Binzen I, Banfer S, Jacob R, Brunotte L, Garcia-Sastre A, Schmid-Burgk JL, Schmidt T, Hornung V, Kochs G, Schwemmle M, Klenk HD, Weber F: **Influenza virus adaptation PB2-627K modulates nucleocapsid inhibition by the pathogen sensor RIG-I.** Cell Host Microbe 2015, **17**(3):309-319.

23. Kato H, Takeuchi O, Sato S, Yoneyama M, Yamamoto M, Matsui K, Uematsu S, Jung A, Kawai T, Ishii KJ, Yamaguchi O, Otsu K, Tsujimura T, Koh CS, Reis e Sousa C, Matsuura Y, Fujita T, Akira S: **Differential roles of MDA5 and RIG-I helicases in the recognition of RNA viruses.** Nature 2006, **441**(7089):101-105.

24. Hoffmann E, Stech J, Guan Y, Webster RG, Perez DR: **Universal primer set for the full-length amplification of all influenza A viruses.** Arch Virol 2001, **146**(12):2275-2289.

25. Mizushima S, Nagata S: **pEF-BOS, a powerful mammalian expression vector.** Nucleic Acids Res 1990, **18**(17):5322.

26. Guo L, Wang L, Yang R, Feng R, Li Z, Zhou X, Dong Z, Ghartey-Kwansah G, Xu M, Nishi M, Zhang Q, Isaacs W, Ma J, Xu X: **Optimizing conditions for calcium phosphate mediated transient transfection.** Saudi J Biol Sci 2017, **24**(3):622-629.

27. Oh SW, Onomoto K, Wakimoto M, Onoguchi K, Ishidate F, Fujiwara T, Yoneyama M, Kato H, Fujita T: **Leader-Containing Uncapped Viral Transcript Activates RIG-I in Antiviral Stress Granules.** PLoS Pathog 2016, **12**(2):e1005444.

28. Mibayashi M, Martinez-Sobrido L, Loo YM, Cardenas WB, Gale M,Jr, Garcia-Sastre A: **Inhibition of retinoic acid-inducible gene I-mediated induction of beta interferon by the NS1 protein of influenza A virus.** J Virol 2007, **81**(2):514-524.

29. Rajsbaum R, Albrecht RA, Wang MK, Maharaj NP, Versteeg GA, Nistal-Villan E, Garcia-Sastre A, Gack MU: **Species-specific inhibition of RIG-I ubiquitination and IFN induction by the influenza A virus NS1 protein.** PLoS Pathog 2012, **8**(11):e1003059.

30. Gack MU, Albrecht RA, Urano T, Inn KS, Huang IC, Carnero E, Farzan M, Inoue S, Jung JU, Garcia-Sastre A: **Influenza A virus NS1 targets the ubiquitin ligase TRIM25 to evade recognition by the host viral RNA sensor RIG-I.** Cell Host Microbe 2009, **5**(5):439-449.

31. te Velthuis AJ: **Common and unique features of viral RNA-dependent polymerases.** Cell Mol Life Sci 2014, **71**(22):4403-4420.

32. Wang W, Riedel K, Lynch P, Chien CY, Montelione GT, Krug RM: **RNA binding by the novel helical domain of the influenza virus NS1 protein requires its dimer structure and a small number of specific basic amino acids.** RNA 1999, **5**(2):195-205.

33. Marc D, Barbachou S, Soubieux D: **The RNA-binding domain of influenzavirus non-structural protein-1 cooperatively binds to virus-specific RNA sequences in a structure-dependent manner.** Nucleic Acids Res 2013, **41**(1):434-449.

34. Garcia-Sastre A, Egorov A, Matassov D, Brandt S, Levy DE, Durbin JE, Palese P, Muster T: **Influenza A virus lacking the NS1 gene replicates in interferon-deficient systems.** Virology 1998, **252**(2):324-330.

35. Schneider J, Wolff T: **Nuclear functions of the influenza A and B viruses NS1 proteins: do they play a role in viral mRNA export?** Vaccine 2009, **27**(45):6312-6316.

36. Fortes P, Beloso A, Ortin J: **Influenza virus NS1 protein inhibits pre-mRNA splicing and blocks mRNA nucleocytoplasmic transport.** EMBO J 1994, **13**(3):704-712.

37. Marion RM, Zurcher T, de la Luna S, Ortin J: **Influenza virus NS1 protein interacts with viral transcription-replication complexes in vivo.** J Gen Virol 1997, **78 (Pt 10)**(Pt 10):2447-2451.

38. Hatada E, Saito S, Okishio N, Fukuda R: **Binding of the influenza virus NS1 protein to model genome RNAs.** J Gen Virol 1997, **78 (Pt 5)**(Pt 5):1059-1063.

39. Takizawa N, Momose F, Morikawa Y, Nomoto A: **Influenza A Virus Hemagglutinin is Required for the Assembly of Viral Components Including Bundled vRNPs at the Lipid Raft.** Viruses 2016, **8**(9):249. doi: 10.3390/v8090249.

40. Robb NC, Chase G, Bier K, Vreede FT, Shaw PC, Naffakh N, Schwemmle M, Fodor E: **The influenza A virus NS1 protein interacts with the nucleoprotein of viral ribonucleoprotein complexes.** J Virol 2011, **85**(10):5228-5231.

41. Karlas A, Machuy N, Shin Y, Pleissner KP, Artarini A, Heuer D, Becker D, Khalil H, Ogilvie LA, Hess S, Mäurer AP, Müller E, Wolff T, Rudel T, Meyer TF: **Genome-wide RNAi screen identifies human host factors crucial for influenza virus replication.** Nature 2010, **463**(7282):818-822.

42. Nturibi E, Bhagwat AR, Coburn S, Myerburg MM, Lakdawala SS: **Intracellular Colocalization of Influenza Viral RNA and Rab11A Is Dependent upon Microtubule Filaments.** J Virol 2017, **91**(19):e01179-17. Print 2017 Oct 1.

43. Mouland AJ, Mercier J, Luo M, Bernier L, DesGroseillers L, Cohen EA: **The double-stranded RNA-binding protein Staufen is incorporated in human immunodeficiency virus type 1: evidence for a role in genomic RNA encapsidation.** J Virol 2000, **74**(12):5441-5451.

Chapter 6

Acknowledgement

First, I would like to thank Prof. Takashi Fujita who kindly mentored and supported me through my PhD studies. It has been an honour for me to work in Fujita lab. I also thank Prof. Hiroki Kato and Prof. Takeshi Noda for their kind scientific advices and assistances in this project. Furthermore, I thank Dr. Michaela Weber for establishing the VLP system and Dr. Dacquin M. Kasumba for scientific writing advices and data organizations. Finally, I would like to thank Prof. Friedmann Weber for the kind gift of the VLP expression and minigenome plasmids and Mr. L. H. Li and Y. Tsukamoto for scientific editing and proof-reading.

This study was supported by research grants from the Ministry of Education, Culture, Sports, Science, and Technology of Japan: Innovative Areas “Infection Competency” #24115004 (T.F.) and #19H04831 (T.N.)

This thesis is based on material contained in the following scholarly paper:

Tim Wai Sha, Michaela Weber, Dacquin M. Kasumba, Takeshi Noda, Masahiro Nakano, Hiroki Kato and Takashi Fujita

Influenza A virus NS1 optimises virus infectivity by enhancing genome packaging in a dsRNA-binding dependent manner.

BMC Virology Journal 17:107 (2020)